CHALMERS

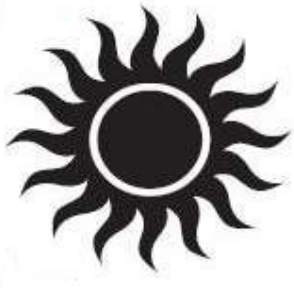

Development of New Spectroscopic Instrument for Enivronmental measurements of gases from industries and volcanoes

Master of Science Thesis

Modris Matisāns

Department of Radio and Space science
Devision of Optical Remote Sensing
CHALMERS UNIVERSITY OF TECHNOLOGY
Göteborg, Sweden, 2010

ABSTRACT

Refineries and petrochemical industries are large point sources of volatile organic compounds. These gases are active in tropospheric chemistry and produce photochemical smog. In order to complement the arsenal of instruments for fugitive gas measurements a new instrument has been developed following a theoretical investigation of a previous master thesis. The new instrument is a so called non dispersive spectrometer which will replace the infrared spectrometer in a solar occultation flux (SOF) instrument, currently used at the Radio and Space department. This new device is aimed to be inexpensive, light weight and robust. In the SOF method gas flux measurements are conducted using the sun as the light source and by observing the amount of light transmitted through the plume of gas. Further, wind speed data are used to determine gas emission flux in mass per time units. In this work the non-dispersive spectrometer was designed, built and tested in the laboratory as well as in the field. In the instrument the sun, from a so called solar tracker, is transmitted through an entrance opening with 2.54 cm in diameter. The light is further transmitted through a filter wheel, with a set of bandpass filters, to a PbSe infrared light sensor that records the varying voltage reading for each filter consequently as the wheel rotates at a speed of 6 to 7 Hz. Thereafter, filter transmittance measurements are used to calculate the alkane column density. The filters are also used to compensate for the presence of water and methane as well as a slope in detector sensitivity over operating region. In a field test, the non-dispersive spectrometer was combined with a solar tracker and positioned on a pickup car. Measurements were then conducted downwind a refinery revealing alkane mixture carbon number of 4.6 and emission estimation of 122 kg/h. This was consistent with SOF measurements that were being conducted in parallel.

KEYWORDS: infrared, gas emission, flux, broadband radiometry, broadband filter instrument, SOF, alkanes, carbon number

PREFACE

As a part of my studies at Gothenburg University, master's program of Atmospheric science, it was tempting to proceed with master's thesis at the department of Radio and Space Science, Optical Remote Sensing group. I thank Johan Mellqvist for welcoming me into both the before mentioned Chalmers group and Fluxsense company group to perform master's work in a truly innovative matter, which is building a new instrument for SOF method.

Jerker Samuelsson is responsible for help in so many aspects of the work that I almost should mention him as a co-author.

Peter Lundin and Håkan Salberg helped me so much in field work,

John Johansson gave me extremely valuable insights in scientific aspects of the device properties that we investigated together,

Brian Offerle answered my questions with in depth analysis that often opened my eyes to aspects neglected before.

Johan Ekholm gave me literally lectures on electronics and very practical issues that were irreplaceable.

My thanks also are directed to Chalmers colleagues from other groups of department for supporting in general questions on instrument building aspects as well as non-work related matters.

I also have enjoyed immense support from the Blumenstein family in Mölndal, who have given me feeling of home all through thesis writing time.

Thank you also to the absolutely greatest mom on Earth, and this time it is not simply a manner of speaking, as well as grandmother and grandfather back in Latvia.

CONTENTS

1. ENVIRONMENTAL INTRODUCTION

Definition of volatile organic compounds is approximate; however, it is described by "volatile" and "organic". European Union official definition states:

"A VOC is any organic compound having an initial boiling point less than or equal to 250 °C measured at a standard atmospheric pressure of 101.3 kPa and can do damage to visual or audible senses."[1]

Health effects of VOCs can be escalated indoors, where concentration values can be a factor of 10 greater than outdoors, while outdoors VOCs are significant players in atmospheric chemical processes. Ground level ozone and acidification issues are treated by setting limit emission values for VOC emissions. Most refineries and a landfills as well as port facilities face routine measurements of the fugitive gasses, which can be later compared to the model predicted emissions. Such gasses as alkanes, alkenes and aromatics are of particular interest due to their highly active participation in daytime and night-time atmospheric chemistry. Measured values very often exceed model predicted values, thus, often it is essential in discovering leakages. Not only measurement interest is driven by environmental issues, in most cases a leak also implies loss of potential income. Lucky for environment, it serves as a motivation factor for measurements and research.

VOC gasses are natural constituents of atmosphere, but human emissions alter their quantity and spatial distribution. The sites under influence of altered consistence of atmosphere shall undergo altered atmospheric chemistry and to understand it thoroughly it is necessary to keep track of anthropogenic emissions of these gases.

Types that constitute greater portion of VOCs are alkanes, alkenes and aromatics. Alkanes are non-cyclical hydrocarbons with a general chemical formula C_nH_{2n+2}. In alkanes only single C-C bond is present. Alkenes are non-cyclical hydrocarbons with at least one double C=C bond with a general chemical formula C_nH_{2n}. Aromatics are the cyclical hydrocarbons that may have any sort of carbon bonds. Since single, double and triple carbon bonds all have different resonance frequencies in IR range of electromagnetic radiation it becomes possible to distinguish between these two large groups of VOC in IR light absorption analysis. The aromatics are amazing molecules since merely electronic bonds would not be capable of holding a benzene ring together; however it is due to the delocalized electron rings that accomplish the task. As the ring is kept together with help of another effect apart from electronic bonds, the resonance frequencies of the electron bonds are also shifted to higher frequencies as compared to alkane or alkene single or double carbon bonds.

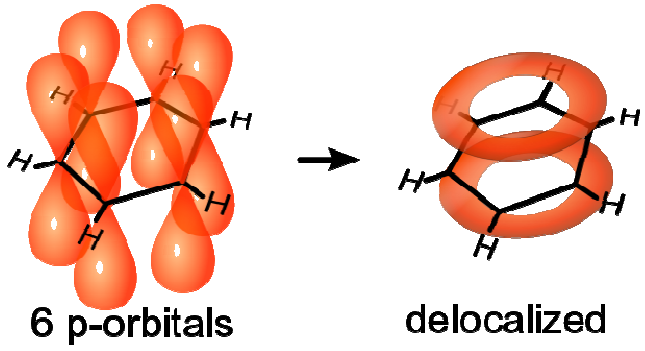

Figure 1 Graphical explanation of how the 6 p-orbitals form delocalized electron rings in benzene (one of aromatics) molecule. [4]

One example of altered atmospheric chemistry due to elevated emissions of VOCs and maybe the most dangerous one is the photochemical smog. This phenomenon was first described in the 50ies, when megacities grew big and automated enough to form such atmospheric effect. The chemical process takes VOCs (anthropogenic emissions), NO (anthropogenic) and sunlight to produce ozone (O_3) and NO_2. Because of its highly oxidising properties tropospheric ozone is harmful for biosphere. The smog becomes visible as a yellowish haze mainly due to NO_2 and also secondary aerosols that are further on formed from these precursors. The chemical reactions are described below considering presence of atmospheric oxygen O_2.

A. **VOC** + OH -> RO_2 + H_2O
B. CO + OH -> HO_2 + CO_2
C. RO_2 + **NO** -> VOC +HO_2 +NO_2
D. HO_2 + NO -> OH + NO_2
E. NO_2 + **hν** -> NO + O
F. O + O_2 + M -> **O_3** + M

It seems the only positive effect of this cycle that is obvious is the destruction of harmful CO gas by transforming into a non toxic CO_2.

Importance of VOCs in atmospheric processes also extends to homogeneous nucleation of particulate matter (secondary formed aerosols), which is still not very well understood process and is studied including models of air mass transportation. Therefore, not only emission estimates but also mass emission measurements are vital for further testing of such models.

Besides environmental and economic aspects of fugitive gas effects latest issues also include aesthetic influence onto human life quality through effects of odours. Flux measurements of such organic gaseous compounds are carried out in order to reveal their source.

Uncertainties in measurements and emissions faced nowadays are a matter of concern for the modelling of atmospheric processes. Measurement uncertainties reach as high as 30%, however the discrepancies between modelled emission and measured emission by different techniques (mentioned later in the text) can easily reach as high as a factor of 10. An example of measured and reported emissions of VOCs is given below in the figure.

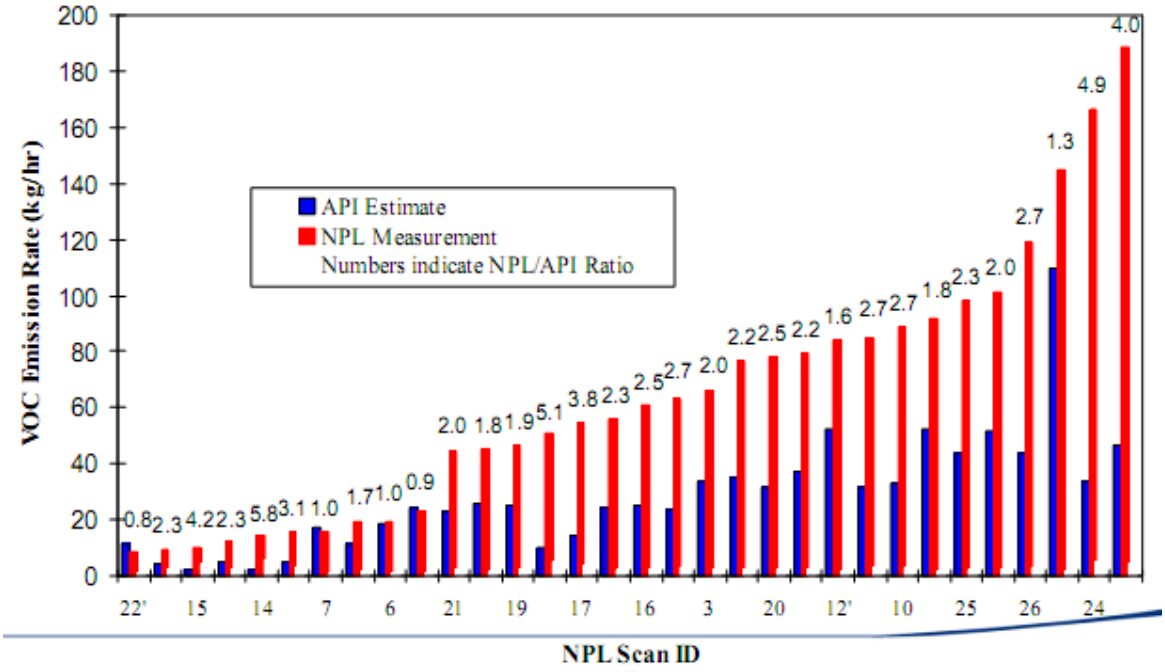

Figure 2 NPL's DIAL measurements (red columns) compared to estimated values of VOC emission flux (blue columns) [image courtesy of NPL].

The graph justifies necessity of VOC measurements since it is an essential link to the reality in the emitting – controlling – modelling - measuring cycle.

2. THEORY OF LIGHT ABSORPTION INSTRUMENTS

2.1. IR spectroscopy

In the heart of most gas measurement techniques there are molecular vibrational energy levels that are altered as a result of interaction with radiation. These are molecular resonance frequencies, which if coinciding with incident radiation frequency or photon energy, can absorb energy of radiation. Molecules further can either remain in the excited state or re-radiate the energy. Re-radiation of energy can take place in any direction differing from initial direction of incident radiation. Thus, the effect of absorption due to atmospheric gasses can be observed.

2.2. Gas Absorption Cross-sections

Assume the general ability of gasses to absorb incident radiation that corresponds to molecule vibrational resonance frequency and corpuscular nature of light. The term "effective gas absorption cross section" means the physical probability of molecule to be hit by a photon, which would result in interaction with a molecule in a process of absorption or scattering. Cross sections for various gasses are determined in laboratories beforehand. These values are describing the probability of a gas molecule interacting with a photon.

2.3. Beer Lambert's Law

General absorption technique mechanism can be described as consisting of light source, light absorbing medium (gas in question) and detector (see fig. X). Detector data is further directed to data acquisition hardware for storage. The physical principles of absorption based measurements are found in Beer-Lamberts law, which states a linear relation of absorbance A to cross-section of gas molecule, number density of molecules N and path length of light l.

$$A = \sigma l N$$

Equipment in nature can measure light intensity in a certain wavelength region(s) and compare it to reference value. Transmissivities (T) of media is defined by ratio of these intensities.

$$T = \frac{I}{I_0},$$

I_0 is the intensity of light before and I – after transmission through media. However, absorbance A and transmissivity T are interconnected with a logarithmic relation

$$A = -\ln(T)$$

As cross-sections of gases have been pre-determined by laboratories, measurements of transmissivity allows for determination of unknown number concentration N.

To add, if the measurement is conducted outside a chamber, estimation of path length *l* can be an essential part of the measurement.

However, in case of high medium optical density τ the measured total gas cross section and gas number concentration N is not linearly correlated as the cross sections are overlapping. In such case transmittance of radiation is close to zero and absorption is said to be saturated. One should avoid measurements in such wavelength ranges.

For atmospheric measurements of several species usually the concept of optical depth or thickness τ is introduced, which is an additive value amongst all absorbers in the light path. It is defined with a wavelength dependant expression:

$$I = I_0 \exp[-(\tau_1 + \tau_2 + \tau_3 + \ldots)]$$

It implies that optical depths of different species sum up to yield the total optical depth of the atmosphere. In spectral analysis this implies that the observed absorption spectrum of sunlight is a superposition of all possible absorbents present.

Since the absorption of molecules is selective as to wavelengths, both in region (IR, VIS or UV) and in lines (absorption lines and bands), measurements can be done by different types of equipment based on these spectral differences. Since hardware, such as light windows, optical fibre, lenses, filters etc., are wavelength sensitive, different techniques not only can but also must be developed to operate in different wavelength ranges.

VOC absorption lines are found in IR range, thus, corresponding equipment can be applied.

3. TECHNIQUES OF VOC MEASUREMENTS

It is essential to distinguish between measurements of VOC concentration and flux. Concentration would be more important in health effect studies indoors and observations of atmospheric chemistry processes. The unit in the case being mass per volume (g/cm3) or parts per million/billion/etc. (ppm, ppb, ppt...). Flux measurements on the other hand measured in mass per time (kg/h), concentration measurement in such case becomes not important since flux can be retrieved directly from gas column. Flux is defined as mass of gas traversing a measurement plane over a unit of time. Geometrically, the plane should be defined that we are interested in. In following subchapters different flux measurement techniques shall be discussed.

3.1. Horizontal flux measurements

In case of VOC emission from a factory, landfill or refinery the horizontal flux is measured, thus, the measurement plane is vertical – as a fence around the emission source or at least on the downwind side of the source if the emission takes place in the direction of the wind and there is no background level input from the upwind side as shown in the following figure.

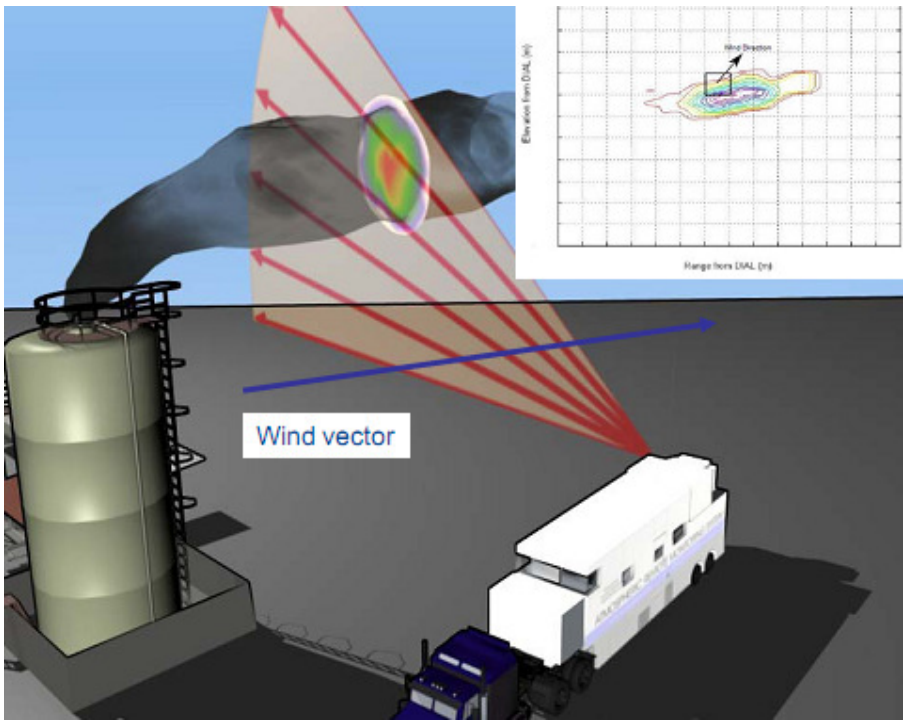

Figure 3 Measurement of a horizontal flux traversing a vertical measurement plane. (example from a DIAL measurement). ~courtesy of National Physical Laboratory, UK.

3.1.1. SOF (Solar Occultation Flux) technique

SOF is a flux measurement method, which observes the sunlight while driving around an emission source. Since this technique is directly applicable with the measurement instrument that is being built during this thesis, it shall be discussed in detail in chapter 4.

3.1.2. DIAL

DIAL – Differential Absorption LIDAR technique [8] implements a pulsed laser beam and scans the sky in a plane perpendicular to Earth. Suppose the emission plume is crossing this plane. By choosing a wavelength that is very well scattered by the gas in question its concentration and distance from receiver can be determined. This technique supports measurements of wide variety of species – VOCs (ethane, methane, methanol and general hydrocarbons), SO2, NO2, NO, Hg, HCl, benzene, toluene, Xylenes with a spatial resolution down to 8 metres.

Data is received in a form of two dimensional profiles. By taking consequent measurements at known wind speed, eventually, the emission flux is determined. To identify the hot spots of emissions horizontal plane scanning can be performed. National Physical Laboratory (NPL) introduces such techniques in DIAL method.

The DIAL principle in distinguishing gases is very handy due to tuning laser capabilities. For certain gas measurement a necessary choice of wavelengths is made in order to eliminate influence of other absorbing species as much as possible. Fig. 4 illustrates the choice of two such handy wavelengths. Subsequently, these wavelengths are compared to each other to determine the differential absorption, which gives the absorbance of gas through the Beer-Lamberts law.

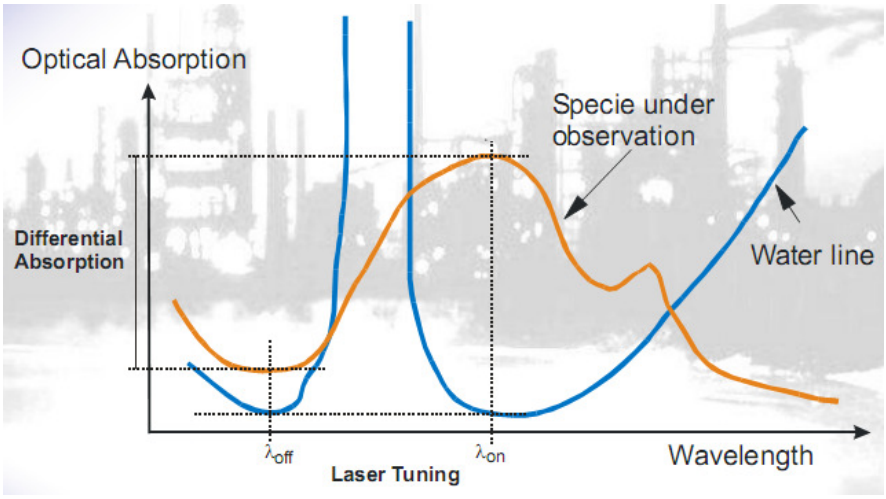

Figure 4 The choice of tunable laser wavelengths in order to eliminate influence of water absorption effects on measurements of specie under observation. (courtesy of Spectrasyne environmental surveying)

Airborne Natural Gas Emission DIAL (ANGEL) is a state of the art technique in scanning the surface of Earth from an airplane for detection and quantification of gas leaks [9].

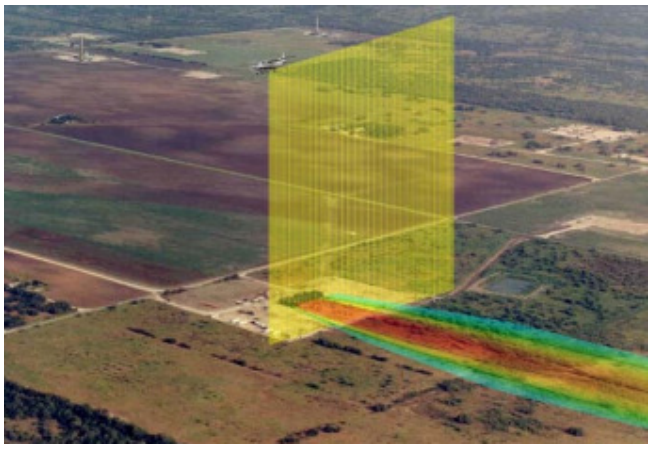

Figure 5 A picture of flying DIAL (ANGEL) measurement straight downwards from the airplane with indicated gas emission plume.

Impressive is the area that can be covered in one day's flight – approximately 1600 km, at swath width available it yield up to 13 square km per day in case of areal observation. The technique is equipped by high resolution mapping camera, DIAL sensor and a digital video camera. These parts are supplemented by heavy and expensive hardware that is installed on the airplane; the technique also requires measurements of steady wind speed at ground level.

3.1.3. DOAS, mobile DOAS, scanning DOAS

The DOAS technique has been successfully implemented in atmospheric monitoring over last two decades [13]. It is Convenient since operated at optical and soft UV wavelengths. It implements a spectrometer and analyses the absorption spectra by approximating the absorption curves with absorption curves of separate absorbents. Thus, the technique can measure several species simultaneously with measurement increments up to 1 second. The drawbacks of DOAS lie in necessity of artificial light source, which has to be directed precisely to the receiver from a distance of several hundred meters. Also, since installation of DOAS equipment requires serious effort, it is a rather static type of measurement that can be moved depending on determination of team approximately once a week.

DOAS technique is implemented in line measurements in urban and rural environments of importance to humans. The technique can be introduced to fence line measurements to estimate gas fluxes; however, such attempts are heavy weight unreliable solutions as these line measurements do not account for cases of large mixing layer heights, thus measure only on ground level.

However, such derived methods as mobile DOAS and scanning DOAS have rendered the technique useful for flux measurements. In such cases the DOAS is transformed to a passive system that, instead of observing artificial light source, observes the

scattered sunlight across the sky.

3.2. Vertical flux measurements

When the emission source is the soil, vegetation, snow or when there is no wind to carry flux in horizontal direction – vertical flux measurement techniques are implemented. Vertical emission or deposition over a large area is a vertical flux measurement. In such case the plane that the flux is traversing is set to be horizontal.

3.2.1. Eddy Covariance method

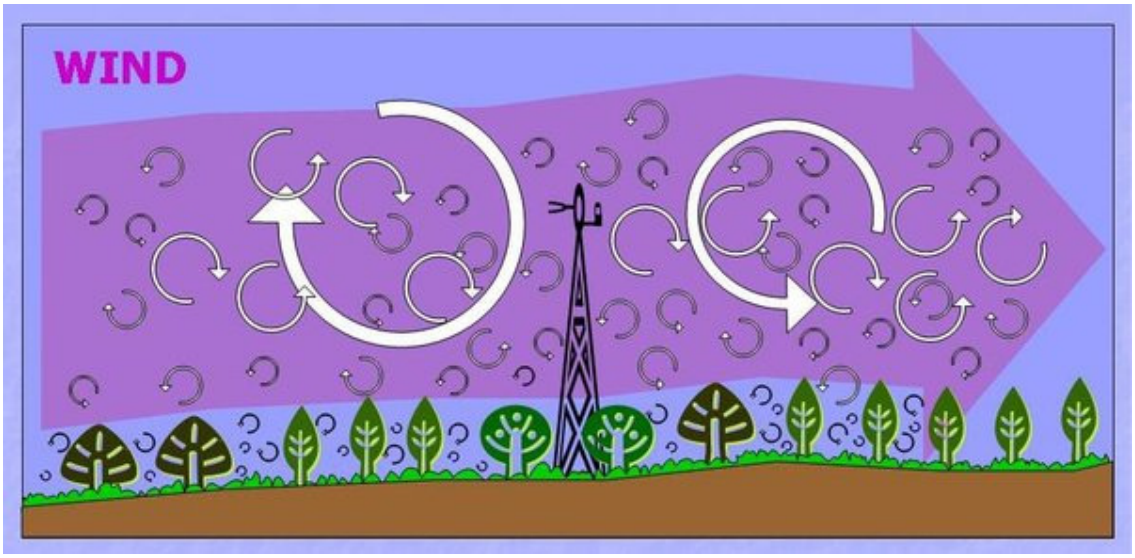

Figure 6 Eddy covatiance measurement schematics. Tower for various altitude gas concentration measurements and eddies above canopy.

Eddy correlation flux measurements [10] are conducted particularly in environments where vertical gas flux is of interest or most prevalent as a result of no strong horizontal winds. Such cases are agricultural gaseous compound flux measurements, where natural cycles are studied and forest areas, where wind patterns are far more complex due to natural obstacles as trees and surface shapes. For eddy correlation flux measurements mostly *in situ* equipment is implemented at two or more heights. Ultrasonic anemometers are implemented for three dimensional wind measurements as these anemometers handle values well below conventional cup anemometers and measure wind speed with accuracy down to 1 cm/s. Therefore with value data base gradients of measured gas flow can be determined over longer periods of time.

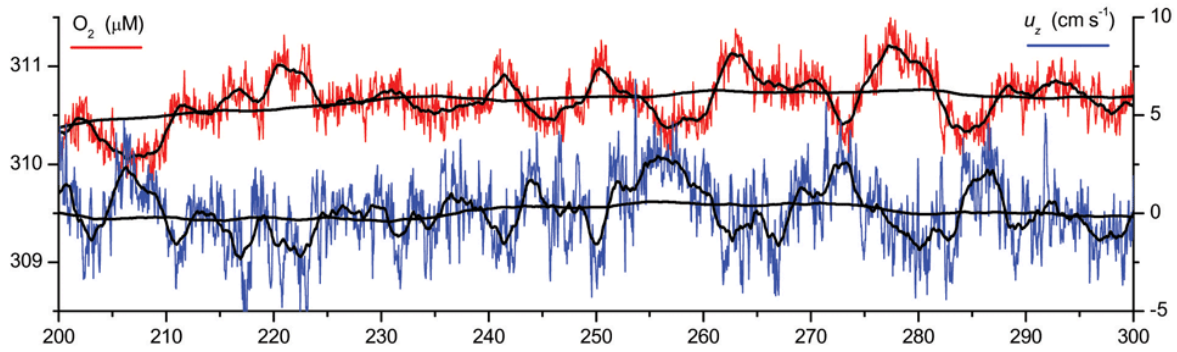

Figure 7 Eddy correlation dataset example where concentration (O_2 in this case) of gas is measured simultaneously with vertical wind speed.

As seen in the example above correlation between upward wind direction and smaller concentration values is obvious. Further, from these measurements the flux in mass per time per area unit ($\frac{kg}{h \cdot m^2}$) of gas in question is retrieved according to general expression:

$$Flux = Windspeed \times IntegratedColumnDensity$$

3.2.2. Box method

When emission rate from a surface is not as high the Box technique can be implemented. The flux in this case is retrieved from measuring the actual concentration of the gas inside a confined box that is constructed above the emitting source. By analysing the time series of concentration measurements allows for flux retrieval. Of course, such method is very intrusive, since it actually measures flux in a confined space, isolated from natural environment. Nevertheless, for slow flux rates it proves to be a useful technique.

3.3. Gas ratio techniques

Tracer Gas technique is used in cases of turbulent mixing possibility of fugitive and tracer gases. Such tracer gases as N_2O or SF_6 are emitted in the proximity of gas emission spot. Thereafter gases are mixed together by turbulent airflow. Measurement of wind dilution factor is measured and after that multiplied by emission flux rate of tracer gas to obtain the leak gas flux.

Advantage for conducting tracer gas measurements is that simultaneously with measurements of observed species the mixing ratio of tracer gas and gas in question is detected during daytime with Sun tracking techniques, thus rendering it possible to extrapolate the observed species measurement data for temporarily cloudy, overcast or night time conditions.

3.3.1 meFTIR

Open Path Fourier Transform Infrared (OP-FTIR) technique is based on Michelson interferometer scanning the IR wavelengths up to 10 μm [12]. The light beam is split in two so as to guide one beam through a reference medium and the other through the observed medium. Then instead of observing power intensity of wavelengths, the interferogram between these two beams is recorded. By applying Fourier transform onto the interferogram a conventional spectrum is obtained.

Similarly, meFTIR (Mobile Extraction FTIR) technique [11] is performing interference measurement; however, this technique is mobile and contains a white cell that collects sample of ambient gas to analyse necessary species on the travelling vehicle. This mobile *in situ* technique can be complementary to other measurement techniques; besides, it is not weather dependant and can be implemented to monitor the background level gas concentration.

Atmospheric measurements can be performed by *in situ* measurements and remote sensing techniques. *In situ* means placing equipment in the environment that possesses the measured qualities. Remote sensing techniques usually involve receiving information of the environment under study from a distance by interacting with it through a medium as radiation of electromagnetic or sound (pressure) waves. Taking samples and analysing in laboratory can be seen as intermediate state between the two; however, it is usually referred to as *in situ*. When it comes to measurements of gaseous compounds, examples of *in situ* measurements are mobile extractive Fourier transform infrared (meFTIR), chemo-luminescence and photo-acoustic technique. The remote sensing techniques include solar occultation flux (SOF), DOAS (Differential Optical Absorption Spectroscopy), DIAL etc. Further, the main techniques in use today will be discussed.

The SOF technique [7] for measurements of gas flux has been developed based on Solar light spectrum as the light source. The setup consists of low resolution spectrometer mounted on a vehicle and a solar tracker ensuring continuous spectrometer exposure to sunlight. By observing the infrared radiation range with a low resolution spectrometer it is possible to retrieve the gas flux from an emission source by driving around the source in such a way that the measurement path traverses the emission plume. The SOF technique provides a cost effective solution for flux measurements, its measurement plane is flexible as it is defined by vehicle driving path. Wind pattern and plume shape often determine what measurement plane is most adequate. The general scheme of SOF method is described in the following illustration.

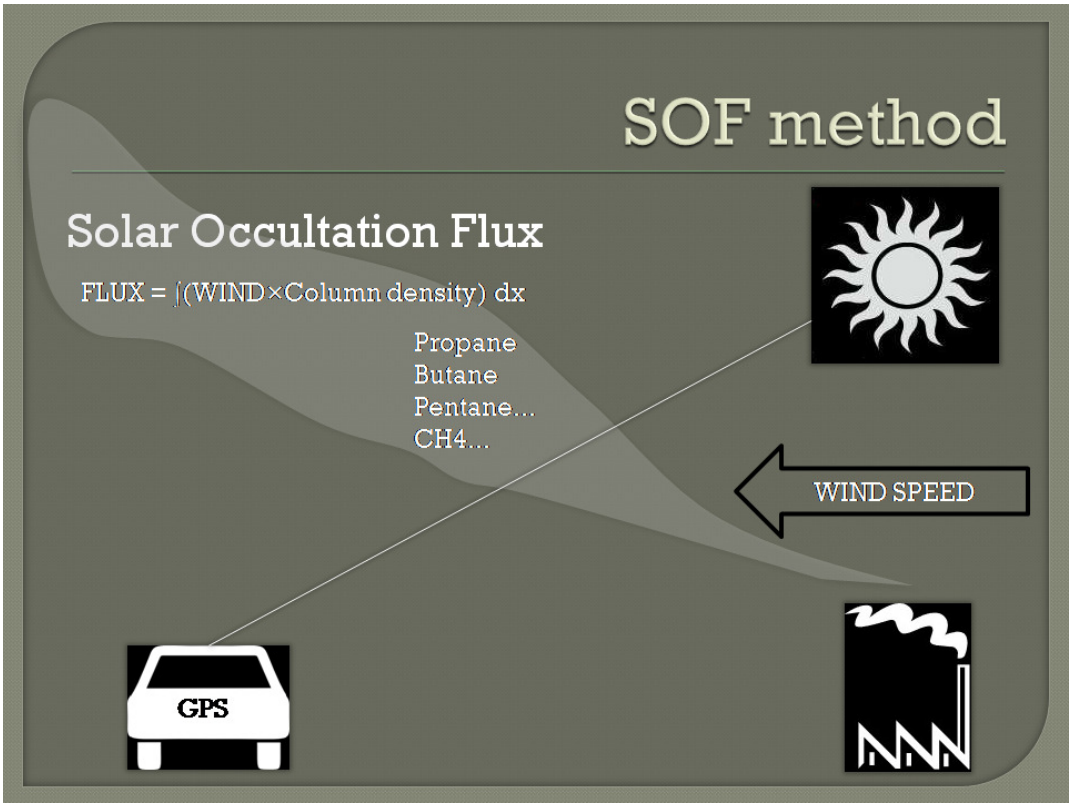

Figure 8 Scheme of SOF method.

As the vehicle with SOF instrument on board is driving approximately orthogonal to the wind direction and observing the sunlight, it is traversing the plume that contains chemical species under question. On board the vehicle a GPS (Global Positioning System) unit records the location of the vehicle as a function of time. Thereafter, by integrating the multiplication of wind speed and retrieved column density of measured gas over the path length driven reveals the flux in mass per time unit (for alkanes usually kg/h).

4.1. Spectroscopy

Infrared spectroscopic instruments are operating within wavelength range of approximately 1.8 to 14 μm but for SOF technique also visible and UV spectral range instruments are used. The measured value is column density of the gas in question (mg/m^2). Since the alkane absorption spectrum has a pattern of two broadband structures (2870 and 2970 cm-1) it is possible to compare these two. The first structure overlaps more with absorption features of other species, while the second is in a much cleaner alkane absorption wavelength range. By calibrating the measurement the first peak can be used to estimate the total alkane column density in the plume, and the second peak would give a possibility to estimate the average weight of alkanes – carbon number, average number of C atoms in alkane molecule since a correlation of carbon number and absorbance ratio between the filters exists.

The narrow bandwidth spectroscopy in NDIR device can be seen as low resolution spectroscopy with focus only on the interesting wavelength ranges, eliminating the rest of light, thereby also improving the signal to noise ratio in measurements.

Most abundant interfering species in the atmosphere is water. In order to compensate for its influence a measurement of water amount is preferable. Since regular water molecules are absorbing too efficiently in the wavelength region above 3000 cm-1 to be measured by this physical principle, heavy water HDO can be measured. Even though there is 1 molecule per 3200 H2O molecules in the atmosphere it could be sufficient as a result for measuring abundance of water.

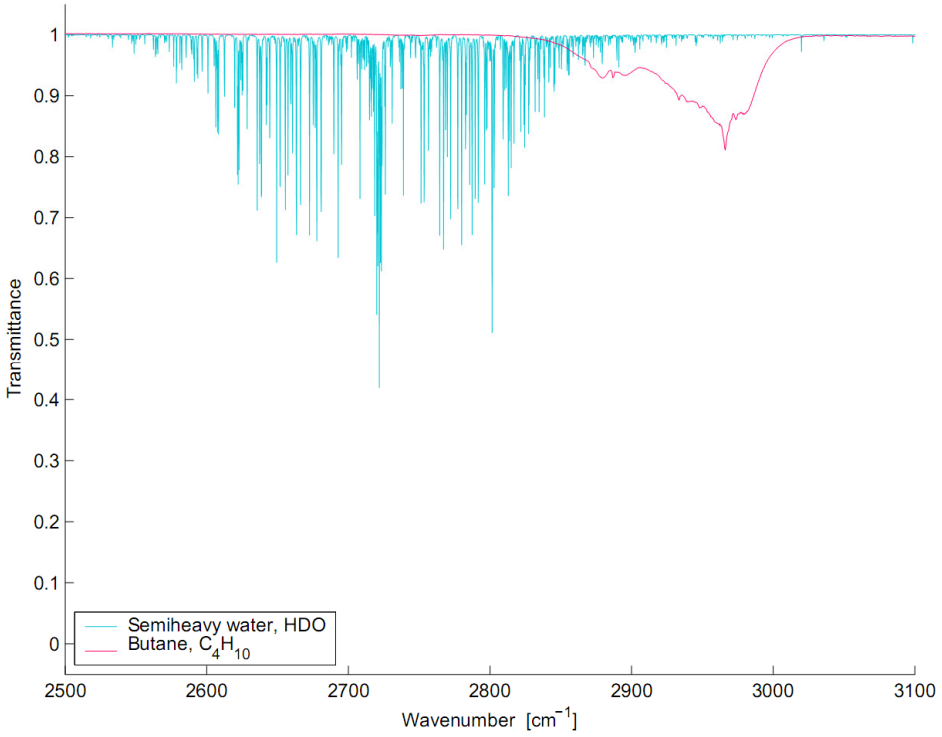

Figure 9 Absorption spectra of semiheavy water HDO and butane C_4H_{10}.

By choosing a reference filter in the wavelength region where HDO absorbs effectively the task of compensating for water might be acheived.

4.2. Measurements

SOF (Solar Occultation Flux) is a gas column concentration measurement technique that uses the Sun as light source. By looking directly into sunlight through a Sun tracker the optical depth of atmosphere with respect to observed species can be determined. Avoiding quantification of concentration values the mass flux of gasses is measured by circling around emission source. As in fence line technique the wind speed measurement, preferably a vertical wind profile is necessary to retrieve the mass flux of emission according to expression:

$$Flux = v \times \int_a^b column_{vertical}(x)dx$$

v – wind speed orthogonal to emission flow,
column$_{vertical}$ – column measured concentration as to vertical measurement,
x – measurement trajectory dimension,
a and **b** – points of trajectory before and after the plume has been traversed.

In SOF measurements the trajectory of measurement is recorded by GPS unit, which is installed on the vehicle. As a result, column concentrations can be displayed on the

map.

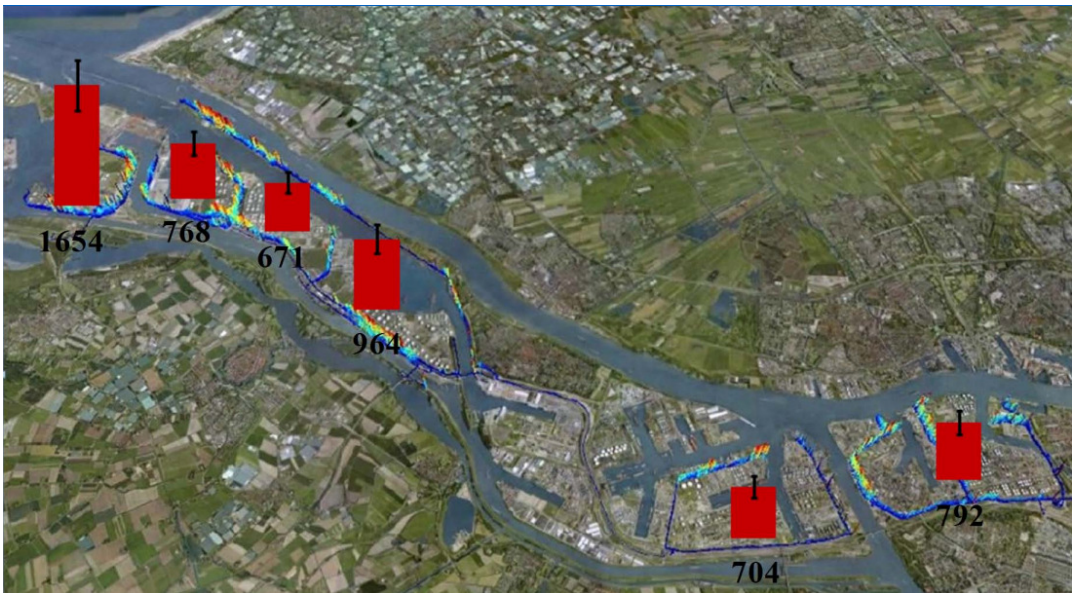

Figure 10 Example of SOF measurements at Rotterdam harbour. Six different areas are circled by SOF technique to determine alkane emissions in kg/h (Mellqvist, Emission Measurements of VOCs with SOF method in the Rotterdam harbour, www.fluxsense.se).

Such SOF measurements are performed in most refineries, landfills and harbours in Sweden on a regular basis, also occasionally including water treatment plants, flares, processing areas and product storage facilities.

By measuring emissions of carbohydrates we can also evaluates efficiency of flare combustion. Since the more efficient combustion the lighter the residual carbohydrates are emitted. This statement can be paraphrased as, for example, ratio between alkanes and alkenes, or single carbon and double carbon compounds. One such attempt has been described in paper [4].

Non-dispersive Infrared SOF (NDIR SOF) is the technique of this work. It performs a gas column concentration measurement based on various narrow IR band pass filters transmittance. Transmittance values are thereafter compared so as to deduct the gas column concentration values.

5. HARDWARE

5.1. Design of the optical filter instrument

A criterion that was important and was to be chased in design is lightweight construction and mobility of the device. As a result in approximate dimensions of 200X120X80mm the following parts were compiled.

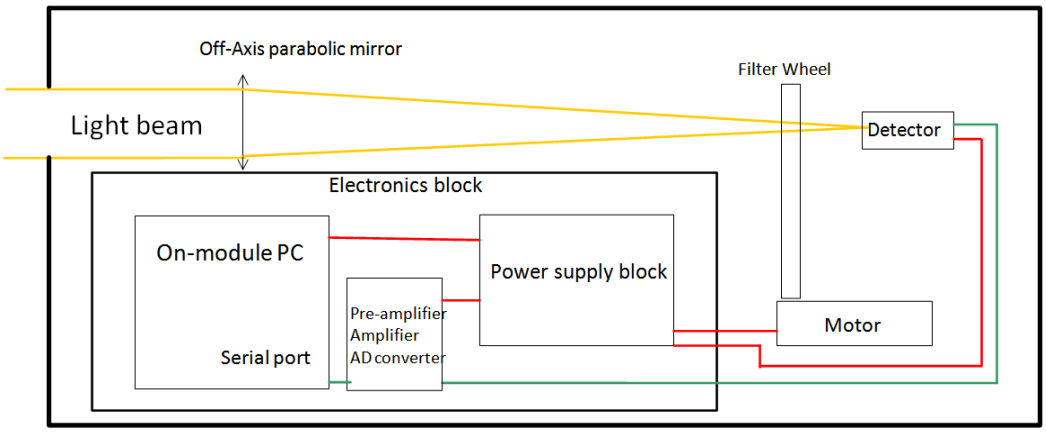

Figure 11 General scheme of design of the optical filter instrument.

The light beam enters instrument through a 1 inch diameter hole directly from the solar tracker. Since IR light is used, optical parts are mirrors instead of lenses that are bad choice in this region due to general high absorbance of optical light transmitting materials. Light is reflected off the off-axis parabolic mirror to be focused on the sensor surface of 1 mm^2. Before the light hits the sensor it is guided through a filter wheel that contains 6 filter positions. At the moment of transferring through the filter, light beam diameter should not be greater than 5 mm in order to ensure that light is transmitted through one filter and one filter only for some period of time that is further defined by the speed of data acquisition from the filter, and also the speed of rotation of the filter wheel.

Filter wheel speed is determined by the speed of rotation of the motor (rpm) and by the radius ratio which can be adjusted to alter the eventual rotational speed of the wheel. Achieved rotational speed is approximately 500 rpm.

Signal obtained by the detector is then delivered to electronics block, particularly – preamplifier, and amplifier. The signal is amplified approximately 10 000 times, thus both amplifiers are used. After signal has been amplified to range of 0 to 5 V, it can be digitalized though AD converter. A 16 bit AD converter suffices as it provides 2^16 levels of voltage steps for measurements.

Thereafter, the digital data is delivered to a computer that performs data storage,

analysis and data validation procedures. For the purpose an on module PC can be implemented to render the device capable of standalone functionality. However, this option has not been implemented currently due to high computing power requirements of the used MatLab software.

In order to decide about the optical design of the device some light-filter interaction effects had to be considered and investigated. Firstly, the choice had to be made between a narrow collimated beam and a focused light beam. If collimated beam is directed to the sensor then the position of sensor can be adjusted only in two dimensions. In case of focused light beam – care should be taken for the focal length at which the sensor is to be positioned.

A three dimensional design of the instrument, its dimensions and relative placement of main parts is presented in Appendix IV. According to this design the instrument was produced.

5.2. Motor and Wheel

The choice of motor is directly dependent on two basic parameters of the wheel and its construction.

Firstly, the type of wheel driving solution was chosen. Initially, as seen from the prototype a central driving construction was considered, however, in order to maximize the endurance and roughness properties of a motor it was decided to drive the wheel tangentially, with a motor placed at the outer surface of the spinning wheel, thus, taking the burden of the weight of the wheel away from motor. This construction would save the trouble of wearing out the axis holding fastening due to acceleration and deceleration.

Secondly, power of the motor necessary is to be determined. Power was intentionally minimized to 0.75 W (0 – 6 V), which would fully allow to run the motor on a 3 V battery. Thus, the heat dissipation of motor was minimized to minimize internal temperature of the device, thus, also the burden on cooling of the sensor would be minimized.

Investigation of possible designs of wheels was carried out using Solid Works hardware engineering software. Appendix I reveal the prototype of wheel that was later dismissed due to excessive number of parts. It was considered since its simplicity of having only one wheel part in the middle that would hold three filters on each side fastened by support structure requiring six additional fasteners each held by two screws to the wheel.

Instead simplified design was created (Appendix II). The weight of such construction was estimated around 22 grams with density of aluminium for wheel

parts and density of glass for filters. Further, in Appendix III the manufactured wheel by parts are presented.

5.3. Sensor

For minimizing the size of the device and ensuring ease of use PbSe sensor was chosen as its responsivity characteristics correspond to the necessary IR region (3 – 4 μm) to be observed by NDIR SOF device. The spectral response vs. wavelength is depicted in the following graph.

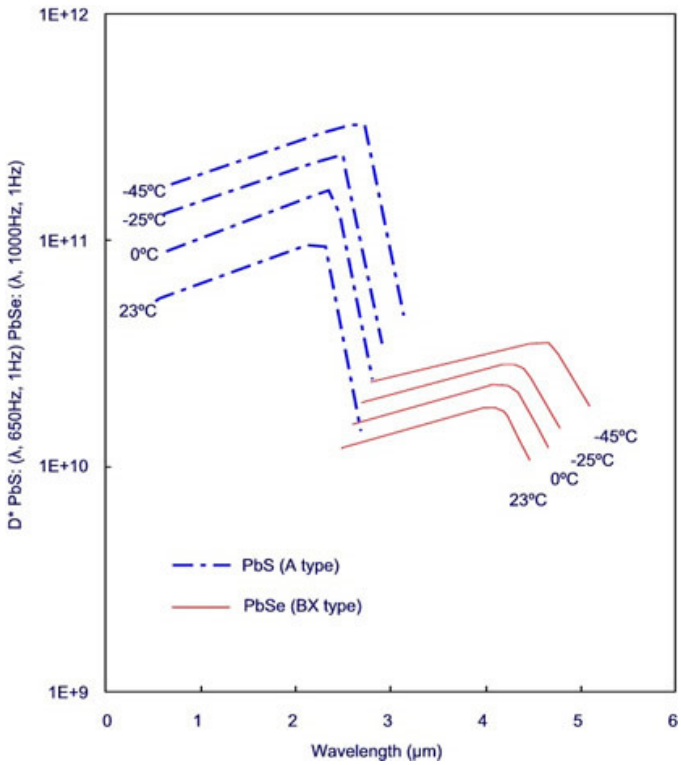

Figure 12 Sensor spectral response curves for various temperatures (PbSe).

The PbSe infrared sensor is cooled thermoelectrically by a Peltier element. This allows for temperature decrease of up to δT = -60°C. Thus, assuming the room temperature of +25°C it is possible to achieve -35°C operating temperature. Considering the responsivity vs. temperature curve (figure 13) we are well in high responsivity range.

Another parameter worth mentioning is the incident power sensitivity of detector. The following illustration tells that for the application we should not go over 10 μW/mm^2 of incident radiative power, as beyond this limit detectors responsivity is no longer linearly related to the measured radiation.

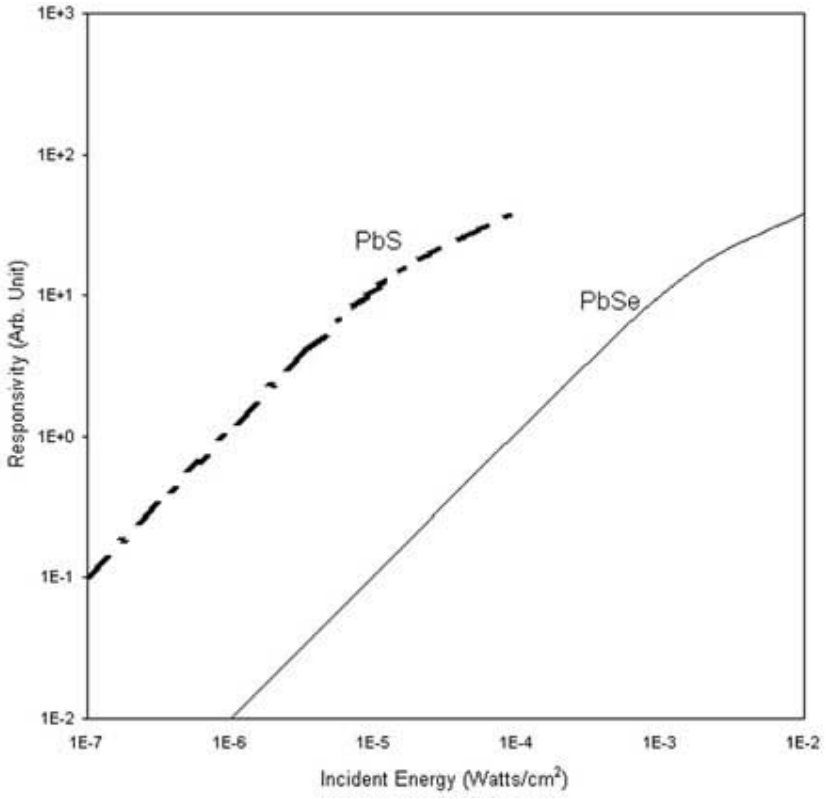

Figure 13 Sensor linearity curve (PbSe).

The radiation power range can be estimated in the following way to check if the threshold of 1 mW shall be exceeded:

Entrance diameter d_0 = 2.54 cm
Entrance area S = 5.07 cm^2
Filter FWHM = 26 ~ 68 cm-1
Filter example CWL = 2800 cm^{-1} = 3.57 µm
At these wavelengths the solar irradiance at sea level is I_{sol} = 14 $\mu W/cm^2 cm^{-1}$

Thus, range of incident power of radiation through filters is 0.0364 ~ 0.0952 mW/cm^2, which for 5.07 cm^2 of entrance area yield 0.182 ~ 0.476 mW power incident on the sensor assuming that all of incoming radiation is successfully focused on the area of sensor (1 mm^2). Naturally, it would not be the case practically. Thus, we should be on the safe side for the given amount of light, though special attention should be paid to excess light dispersed inside the device and absorbed in filters, as to not change optical properties as a result of overheating. For this purpose use of cold mirror on the entrance of optical instrument is intended in order to cut off optical wavelength region of sunlight.

Sensor requires power of up to 0.25W at 0.5V and provides fast response time of 3 to 5 µs, which again allows for high rotation speeds of the filter wheel if necessary.

Very useful and convenient is the inbuilt thermal resistor that if needed can be used to monitor the temperature of sensor to correct for its effects.

5.4. Amplifier

To amplify a signal from 0 ~ 500 μV to the range of 0 ~ 5 V, the total amplification gain G necessary is 10 000. Commercially available differential preamplifier was used that can be adjusted by a resistor R according to expression $G = 1 + \frac{50k\Omega}{R_G}$ (since INA128 model was implemented).

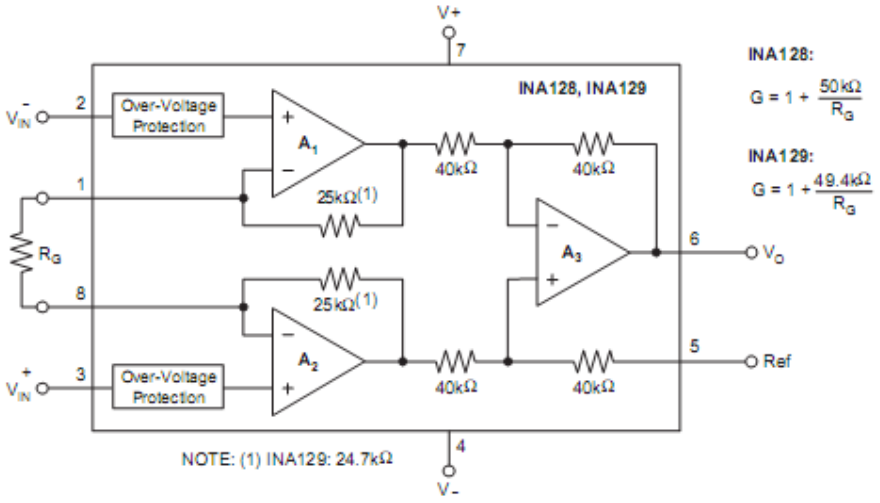

Figure 14 Circuitry of preamplifier and equation (INA128) for calculation of gain G.

Since by approaching the maximum amplification of 10 000 times with this appliance the frequency response decreases (see fig. 5) it was necessary to apply also a secondary amplifier. For this use the amplifier TL064 circuit was used.

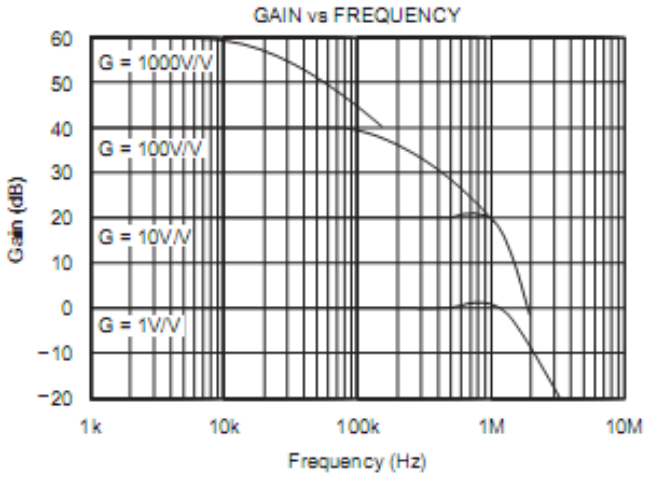

Figure 15 Frequency cut off curves as a function of gain of preamplifier.

Secondary amplifier tuned to a fixed gain G was introduced as follows in figure 16.

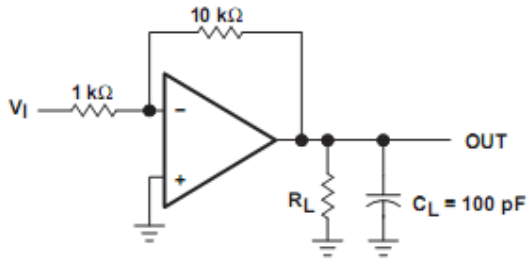

Figure 16 Circuitry of secondary amplifier with fixed gain of 10.

Total gain over amplifiers is the product of each amplifier in series. Thus, by having secondary amplifier fixed we can alter gain by a single resistor RG at the preamplifier. This low pass filter is better to be implemented on the secondary amplifier since it would not influence the amplification factor.

In order to get rid of high frequency noise a capacitor C can be placed in parallel to the resistor R connecting negative input and exit of amplifier (10kΩ in figure 16), thus frequencies higher than f are cut off:

$$f = \frac{1}{RC}$$

5.5. AD converter

Analogue Digital converter converts the amplified analogue signal of the sensor into digital further to be delivered to data acquisition hardware via the serial port. The wheel contains 6 filters. Filters are also overlapping. Possibly for further work the overlapping parts can be used as well as hybrid filter types or as dark reference, thus, in total there are 12 different areas but 3 of them are obscured by the wheel construction, which is not important in this calculation. If the wheel is rotating at speed of 10 Hz, it guaranties rather good measurement independency of atmospheric fluctuations. Thus, in 1 second the light beam is to traverse on average 120 different filter areas. For each area of filters we would like to have at least 5 to 10 transmittance measurements to calculate the average or be able to omit outlier values if such occur. Thus, approximate minimum required for ADC sampling frequency is 120 * 10 = 1 200 Hz. However, the more the better, as long as it does not overload the data acquisition and analysis system.

Bit rate of the converter is representing how many levels of intensity of signal are distinguished by the converter. Minimum bit rate can be directly determined from signal to noise ratio. This value for worst of the two detectors purchased is 538. Thus, there should be at least as many distinct signal levels. Commercially available AD converters range from 10 to 32 bits. Thus, at 10 bits AD converter:

$$\text{Levels (10)} = 2^{\text{bits}} = 2^{10} = 1\ 024 \text{ and Levels(16)} = 2^{16} = 65\ 536$$

For the necessary application 10 is minimum necessary bit number. Such converters also are allowing for shorter conversion time. The chosen MAX1243 AD converter performs at 5.5 to 7.5 µs conversion time; it would be fast enough to operate at maximum 100 kHz sampling frequency. Also, it possesses standard 3-wire serial interface. Also, higher bitrate AD converters comply with the application needs. 16 bit AD converter was chosen that would allow for distinction of 65 536 levels. Such abundance of measurement levels might seem as oversampling, nevertheless, it allows for deeper insight into behaviour of sensor noise.

5.6. Infrared Band-pass Filters

Interference filters are built to transmit or reflect incident radiation. Some of incident radiation is absorbed, but the total energy balance of transmitted T, reflected R and absorbed A portions yield 100%.

$$T + R + A = 100\%$$

Filters are manufactured in a manner that the incident radiation undergoes the self interference over the volume of filter. The transmitted wavelengths are interfering constructively but the rejected wavelegths interfere destructively and cancel out (Figure 17). In such manner virtually any band-pass filter can be produced by simply altering the refractive indices and/or thicknesses of layers in interference filters [6]. By introducing more than one infterference layer it is possible to eliminate more wavelength regions from transmitted light, thus, designing necessary band-pass filter. However, filter CWL is dependent on incidence angle, but in the following schematic interference filter explanation incidence angle is not zero solely for the purpose of clarity.

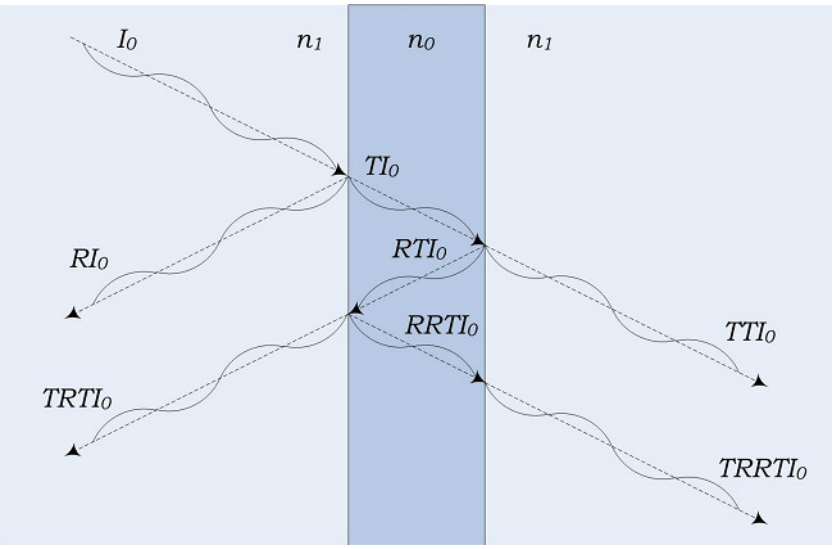

Figure 17 Schematic explanation of interference filter. I_0 – incident radiation, TTI_0 – primary

constructively interfered wave and $TRRTI_0$ – secondary wave that constructively interferes with TTI_0. Other wavelengths interfere destructively. [3]

Choice of filters in this work is based on choice by developers of prototype instrument. Those are 2.54 cm in diameter and 1 mm in thickness. Optical properties of filters are described with full width at half maximum (FWHM) of transmission bands and central wavelength (CWL) of transmission.

In possession such narrow bandpass filters availabe are listed in the following table.

Table 1 Available collection of band-pass filters. Where FWHM is not known, it is to be determined by sepctrometer in further work.

Filter	CWL, nm	CWL, cm^{-1}	FWHM, nm
Alkane 2	3367	2970	57
Alkane 1	3495	2861.2	40
Reference 1	3621	2761.7	42
Reference 2	3759	2660.3	51
HDO	3675.1	2721	71

These filters were chosen by evaluating the absorption features of alkanes, water, methane and semi-heavy water (HDO). Alkane filters are positioned on alkane absorption features. Reference filters are positioned on relatively clean wavelenth regions from absorbances and HDO on 2660 cm^{-1} semi-heavy water absorption pattern.
The planned filter functions and their positions are depicted in the following figure.

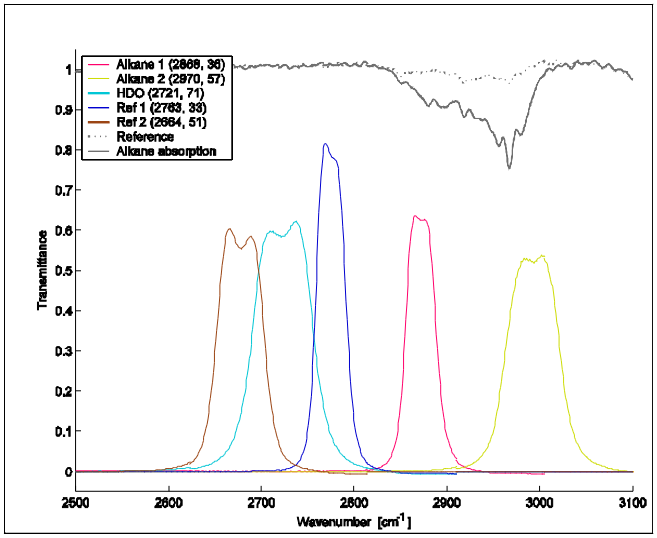

Figure 18 Band pass filter spectra.[3]

Then, assuming these values, influence of varying incedence angle of light onto CWL was estimated. As device has a fixed entrance dimensions of d = 2.54 cm in diamter, the parameter that rather describes the device and determines the maximum

incidence angle φ of light onto filter at the same time is the focal length f of parabolic mirror that is to gather light for the sensor, it served as measure with respect to which the maximum shift in CWL was estimated according to the following expressions:

Incidence angle expressed from light entrance diameter d and focal length of focusing mirror:

$$\varphi = \arctan\left(\frac{d}{2f}\right);$$

Resulting CWL as a result of increase in incidence angle φ:

$$\mathrm{CWL}_{\varphi} = \lambda_0 \cdot \sqrt{1 - \frac{\sqrt{\sin\left(\arctan\left(\frac{d}{f}\right)\right)}}{n_{effective}}};$$

Relative change as to perpendicular case:

$$\text{Decrease in } CWL = \left(CWL_0 - CWL_{\varphi}\right)$$

Implementing Matlab software to analyse value of decrease in CWL the following graph was produced with effective focal length of the mirror on the horizontal axis, since a choice of this value had to be made prior to ordering the part.

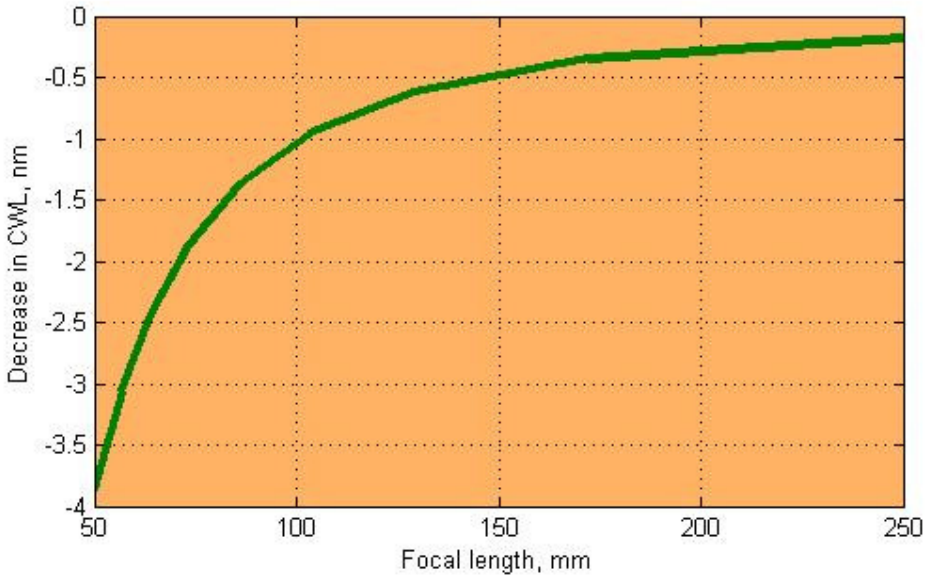

Figure 19 Maximum decrease in transmitted CWL of filters as a function of effective focal length of focusing mirror.

The chosen effective focal length of parabolic mirror for construction is 6 inches = 15.24 cm. It is estimated to have impact on shift of central wavelength of

approximately 0.5 nm. This value for the operating range is negligible.

5.7. Absorption crosssections

For varying background values of methane and/or water the filter signal response in measured absorbance would differ. When gas concentration is zero, the absorbance at increase of 1 ppm of gas shall be greatest, since no or very small number of lines would saturate. However, as column density increases, the saturated absorbance lines would not increase cross section any more as the light transmitted at cretain wavelengths would be zero already. To evaluate effective absorbance crossection (absorbance per ppm increase) variability with respect to different background levels, the gaussian filter functions were applied to transmittances of methane and water spectra (data from Kiruna station). By varying the SZA different realistic column densities of mentioned components were produced. For each column density a perturbation of 1 ppm was applied and the difference registerred. The following graphs summarize results of the quantitative analysis of the background level (expressed in solar zenith angle) influence on cross sections over alkane filters of the instruement.

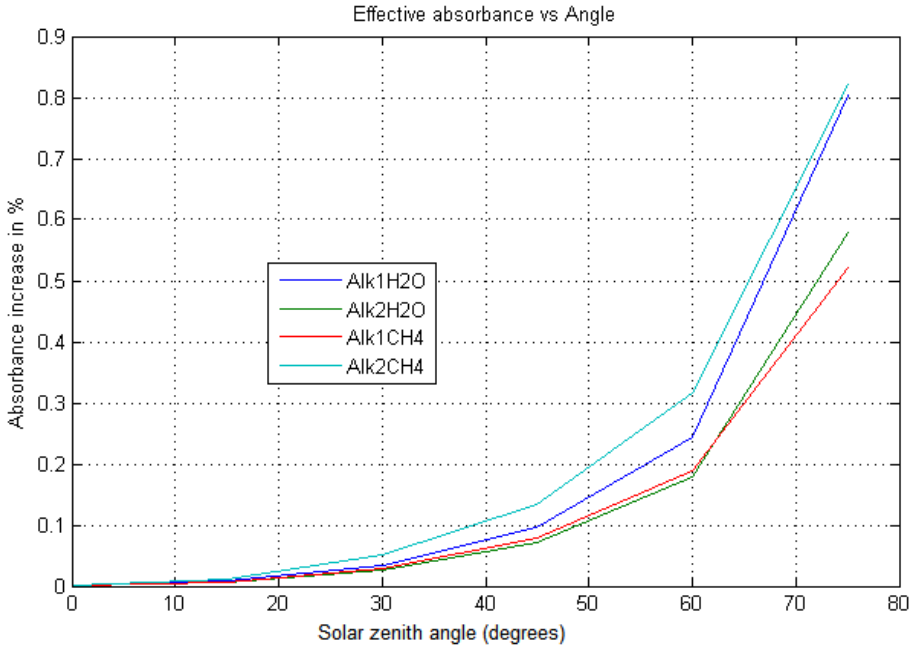

Figure 20 Absorbance increase as compared to solar zenith angle for a constant volume mixing ratio for water and alkane.

As shown in figure 20 the total absorbance measured by filters changes with solar zenith angle. Note that the absorbance values are calculated accounting for saturated lines. This means it is suggestable that measurements are taken around noon and in as short time spans as possible. Regularly in SOF method plume traverse takes up to 15 minutes, a time span during which solar zenith angle does not manage to change considerably, thus, allowing for assumption of constant water

and methane background column density level.

To retrieve filter absorption cross sections filters were measured with a high resolution spectrometer. The obtiained transmittance curves are presented in the following plot.

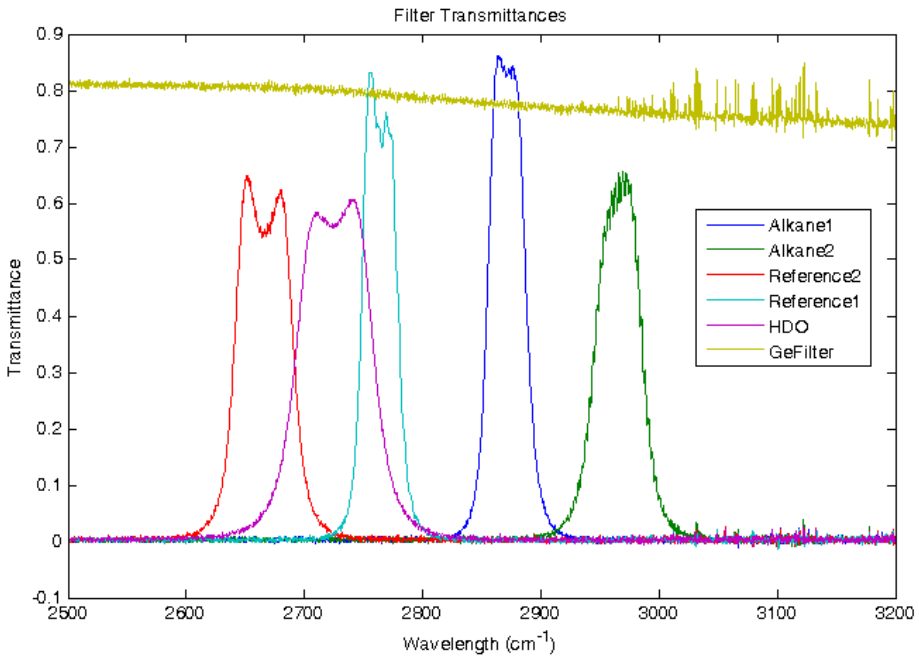

Figure 21 Filter transmittance functions as measured by a high resolution spectrometer.

Thereafter by retrieving the same wavelength region absorbance spectra of all important alkanes (with carbon numbers 3 to 8) and convoluting those with filter transmittance spectra the cross sections were obtained in units of ppm^{-1} m^{-1}. Those were saved in a matrix named SIGMAS, where columns represent alkanes from Propane (carbon number 3) to octane (carbon number 8) and rows – all five narrow bandpass filters in the order - Alkane2, Alkane1, Reference2, Reference1, HDO.

SIGMAS =

1.0e-003 *

0.1350	0.2038	0.2829	0.3421	0.3835	0.3933
0.4683	0.5325	0.6156	0.6702	0.6007	0.5530
0.0090	0.0017	0.0071	0.0097	0.0116	0.0118
0.0141	0.0075	0.0120	0.0143	0.0153	0.0151
0.0095	0.0036	0.0089	0.0111	0.0125	0.0127

First two rows of absorption cross sections were used to calculate their ratio and plot with respect to carbon number of corresponding alkane. Thus, calibration for retrieval of carbon number was performed, resulting in the following graph.

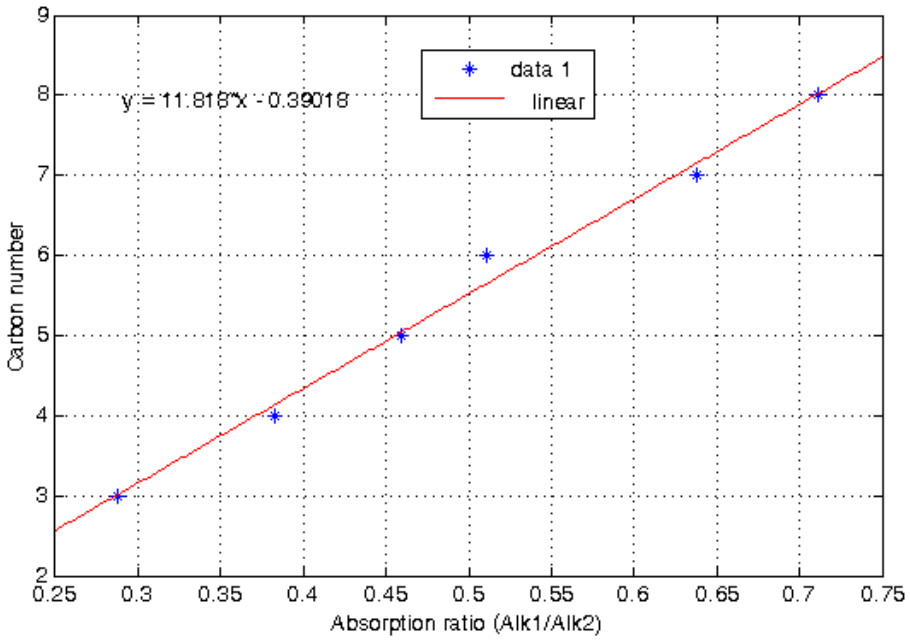

Figure 22 Carbon number as a function of absorption cross section ratios Alkane1 / Alkane2.

Later in measurements this linear correlation was implemented to retrieve the carbon number of the plume alkane mixture.

6. SOFTWARE

In order to acquire data from ADC, retrieve useful information and calculate necessary column density values, a software algorythm was written on Matlab platform. In this section this code and its functionality shall be described.

Firstly, the light optimization code (light_maximization.m) was written to adjust the light beam so that it focuses and falls directly on the sensor area. This was achieved by taking data sample every second of ten values. The median of those ten values for both – sensor light intensity and thermoresistor inbuilt in sensor is displayed on seperate graphs. By looking in the graphs and simultaneously adjusting X-Y parabolic mirror regulator on the instrument the light signal should be maximized to ensure the right optical path geometry. To add, when the thermoresistor would be calibrated to measure real temperature, the value of temperature would be displayed in Celsius degrees or other absolute values. However, during the measurements temperature of the sensor remained rather constant, therefore, was not considered a priority for the time being.

Then the main part of measurement code consists of three main parts:

- Taking background (take_background.m),

- Cutting out each cycle data from data sample for further calculations (cutcycles5.m),

- Retrieval of column density values in ppm*m (retrieval.m).

All three parts of measurement code have been implemented in main m file – gettingData.m. This code file also repeats the take_background.m file if user considers it necessary. Then the code initiates the measurement series with respect to the taken background and draws graphs of the current and previous values calculated. Also, the code stores all data samples in predefined location on hard disk as an ascii, txt file with a name that consists of numbers 'mmDDHHMMSS' representing month, day, hour, minute, second. These files can be referred to later for verification or alternate code implementation on the measurement data.

Since instrument is measuring voltage change proportional to light intensity falling on the sensor I, the measurement of absorbance (A) can be directly made through following expression.

$$A = -\log\left(\frac{\frac{I_{abs}}{I_{REF}}}{\frac{I_{abs,0}}{I_{REF,0}}}\right), \text{where}$$

$I_{abs,0}$ – voltage of Alkane filter, I_{REF} – reference filter voltage, I_{abs} – voltage of Alkane filter during a measurement, I_0 - voltage of reference filter during measurement.

Further code calculates the column density N by dividing Absorbance by effective absorption cross section of alkanes at the wavelengths of correspopnding Alkane band filter (1 or 2).

gettingData.m

Initially the code goes directly to taking the background measurement (**take_background.m**) and after completing that requests permission to contiunue with measurements, if such is not provided – taking background is repeated.

When permission to proceed with measurements is received, the measurement settings are read in through variables of sampling frequency (**samplFreq**), number of seconds for one data sample (**seconds**), number of data samples to be taken until the measurement session is finished. By default **test_rounds** is set to 100, which is a reasonablae number for the measurement graph to be visually comprehensible. Then such formalities as ADC converter port is declared and channel number to be read in memory, followed by setting the previously input sampling frequency and

samples per data trigger is set to ADC operation properties.

When these preliminary settings are input, the measurement session is run in a for loop until test round number (100) is reached. The loop contains trigger command for the ADC along with a **wait** command for reserving time for datasample collection. Right after the data has been taken current PC time is registered and transformed into 'mmDDHHSS' date/time format, where mm –month, DD – date, HH – hour, SS – seconds. Thereafter, a file name is assigned containing this date string to a variable fOut, which then is used to save the raw data sample in a file named exaclty 'mmDDHHSS.txt'. Attention should be paid that if month number is, for example, 5 (May), then file name starts with 5 instead of 05.

As the raw data is saved the code proceeds with algorithm for measurement retrieval. **dataT** is the data set of temperature measurement voltages, located in the second column of each file, and **data** is the filter light intensity voltages.

Next action code is named **cutcycles5.m** since historically it was the 5th significant modification of algorythm for data cutting into periodical cycles of wheel rotation. This I would note as the most critical part of the algorythm, described later on. However, after the data is cut into cycles a monitioring figure is drawn containing several graphs (Appendix V).

First graph depicts each filter voltage measurement behaviour over time along with dark and maximum light leve within a cycle. Second graph contains average values for each filter over their defined data region (in cutcycles5.m) for all cycles detected in the data sample. The rest of the graphs are ceated after **retrieval.m** code has been executed. Third and fourth graphs are calculated absorbance values for each alkane filter along with a slope carrected abosrbance value plot. Fifth graph shows an example of wheel cycle of raw data signal. Sixth graph contains a scatter plot of absorbance (A) or column Density (N) measurement as measured form different alkane filters (Al1 and Al2) demonstrate the comparison between the filters or see a correlation in case of varying measurement values. Relative temperature monitoring graph is represented in seventh plot and carbon number estimates are put down in the eighth graph if absorption values in both filters exceed 0.01, otherwise a value of 0 is recorded signifying that no valid carbon number can be retrieved.

take_background.m

Background taking was chosen to be 4 seconds (bg_seconds), this value should preferably be slightly larger than measurement data sample length to smoothen the variability. In the same manner as measurement data sample taking, the ADC operation settings are input and data collection executed. The median of the second column of background data is denoted as reference temperature (**refT**), and the first column saved as **data**. Thereafter, the **cutcycles5.m** code is executed to cut the signal in wheel rotation cycles. This gives already voltage value arrays for each filter

position containing each seperate rotation cycle to extract the arrays of voltage differences:

```
ref_filter = Ref2 - Z; (reference2 filter value array)
alk2_filter = Al2 - Z; (Al2 filter value array)
alk1_filter = Al1 - Z; (Al1 filter value array)
```

Z is the dark reference value array, it is assigned to the **Black** filter in **cutcycles5.m**.

These arrays are further on implemented to calculate the voltage difference ratio arrays – Al1 and Al2 with respect to Ref2 filter.

There are multiplication factors for Ref2 filter values - 1.3814 for Al2, and 1.2558 for Al1, these arise from integrated filter function ratios, that have been calculated beforehand accounting for the differences between FWHMs and maximum transmittances of filters.

Finally, the median of the voltage difference ratio arrays – the background intensity ratios are stored as **Ibg_Al1** and **Ibg_Al2**. These values are later referred to in **retrieval.m** code as background values. Also, their standard deviation within background data sample is displayed on the Matlab command window to represent the stability of measurement signal to the instrument operator. Thus, these are the values that help the operator to decide if repeated background measurement is necessary.

cutcycle5.m

This code calculates the filter voltage values for each cycle of wheel rotation and the **retrieval.m** code, thus, the retrtieved absorbance and column density values thereafter is most sensitive to these values. Therefore a great deal of attention has been devoted to this part of data validation the algorythm.

Code starts by entering and/or calculatinfg such constants as approximate wheel spinning frequency **spinningFreq, histcutoff** value (used for omitting too long or too short cycles) and **points_per_cycle** are calculated.

From here, the **data** is searched for local maxima and a logical matrix **a** is produced as a result. Then, in a while loop the data is scanned for all maxima that also happen to be above a certain signal threshold. Threshold is defined as:

```
std_thres = max(data) + 0.15*(min(data)-max(data));
```

This expression has been adjusted empirically, so that all cycles in a dataset are detected. Thereafter, all element numbers of the detected maxima are stored in a matrix **new_locs**. Then, difference matrix **difnewlocs** between all neighboring elements of **new_locs** is produced so that in the following step all maxima that would lead to detection of a cycle that is longer than **1+(1-histcutoff)** or shorter than **histcutoff** fraction of the points_per_cycle value are eliminated from **cutcycles5.m** algorithm from this point on. As a result, a maxima element number matrix **new_locs2** is created.

Since starting and ending positions of all useful cycles are registered in **new_locs2**, the cycles are put each in their separate matrices **cycle_X**, where X is the number of a cycle. The following step is determining positions of filters within each cycle. This is done by mathematically defining the cycle as consisting of 6 parts. Position of center for each filter is calculated and then the measured values to either direction from **pos** are taken into account for median value calculation. These median filter voltage values are stored in **FM** (filter matrix); each row corresponds to a different cycle and each column to a different filter.

Empirically comparing signal printouts and calculated values of positions **pos** correction coefficients were introduced to fine-tune exact positions and filter value calculation. Generally, fine tuning was aimed towards more stabile filter voltage value retrieval.

These variable arrays of filter values from **FM** matrix are stored in Al2, Al1, Ref2, Black, Ref1 variables for further measurement retrieval algorithm.

retrieval.m

cP, **cB** and **cO** are corresponding percentages of gas mixture for Propane, Butane and Octane. **propane1**, **butane1**, **octane1**, **propane2**, **butane2** and **octane2** are corresponding gas absorption cross sections for filters **Al1** and **Al2**. From the above mentioned values the absorption cross sections for each filter **sigma_alk1** and **sigma_alk2** are calculated. Finally, a constant **path** is the path length that should be different in case a gas concentration is to be retrieved for a known path length chamber.

Reference filter voltage, Al1 and Al2 filter voltages for current measurement are calculated by subtracting corresponding values from dark (Z). Then Absorbance for each filter is calculated by:

```
A = -log10(ratio_array./Ibg_Al2);
```

Where voltage ratio array is calculated in an analogous manner as for **take_background.m** and Ibg_Al2 is the background is the voltage difference ratio array taken from background measurement.

After absorbance calculation, column density is retrieved by dividing its value by absorption cross section of corresponding filter for the above predefined alkane mixture:

```
N_Al2corr = A./sigma_alk2;
```

To add, error bar is produced by calculating standard deviation of calculated column densities within one dataset of several detected cycles (typically 10 to 15).

All column density measurements are consequently stored in a matrix as element **iii**, which is then represented in **Appendix V** within **gettingData.m** procedure as described in the corresponding section above.

Code was written for two different implementation cases – real time measurements and data re-evaluaion case. Major differences between the codes are that in after validation version requests input of time period to validate in the format 'mmDDHHSS' and then procedes with the same routine as real time measurements but this time retrieving data from files instead of ADC.

7. MEASUREMENTS AND RESULTS

The following graph was produced by altering the applied voltage to the motor by an external power supply in order to approximately determine what spinning frequency to expect by applying certain voltage. The measurements of frequency were done by observing signal in an osciloscope. Obviously, the obtained data points nearly flawlessly comply in a linear relation. 2 Volts was the minimum voltage necessary for the wheel to overcome static friction.

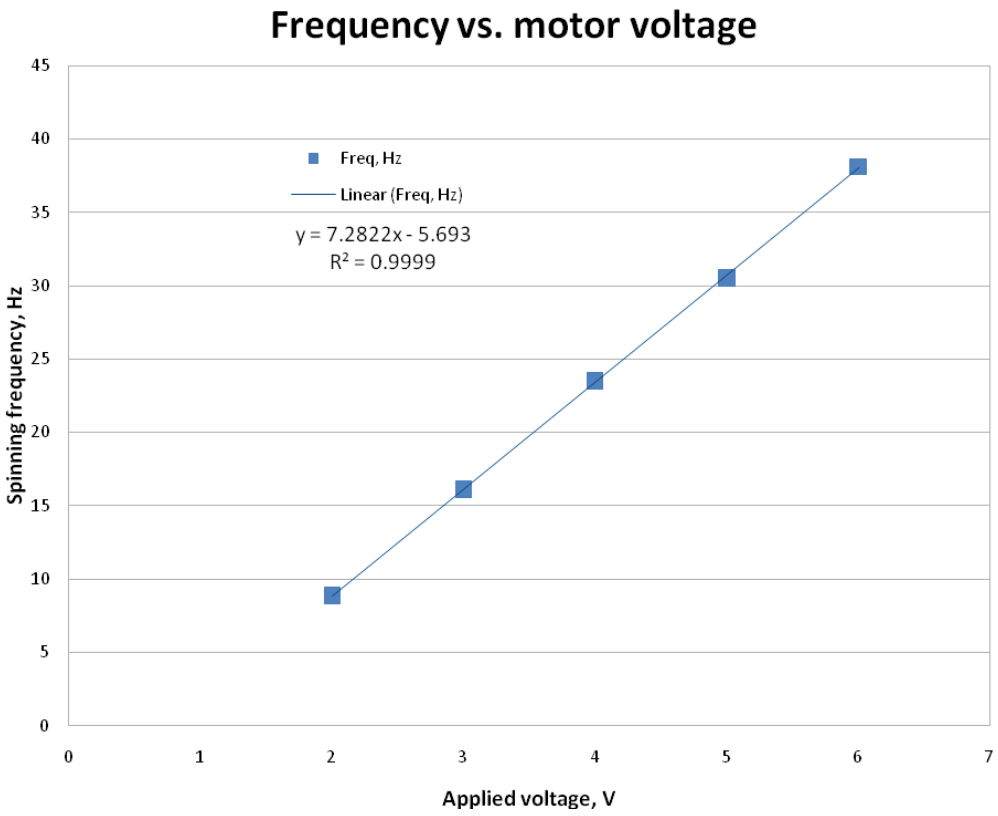

Figure 23 Wheel spinning frequency as a function of applied voltage to the motor.

As a result, for measurements one battery of AA type was considered enough for continuous rotation of the wheel; that produced spinning frequency of approximately 5 to 7 Hz. Even though the static friction occasionally is not overcome by the motor itself, it might require a little push in the beginning, the choice of lower spinning frequency was justified by thus increased number of

points per filter measurement, which increases the signal to noise ratio.

Data sampling frequency by ADC was tested for 10 000, 5 000, 1 000, 500 and 100 Hz sampling frequencies. On the one hand, the sampling frequency was to be minimized in order to minimize the data amount of a sample, which is directly connected to calculation time. On the other hand the sampling rate had to be high enough to register at least 5 data points for each filter level measurement. Eventually, 5 kHz sampling frequency was chosen as it guaranteed around 40 data points for each filter position for later averaging and 333 KB of data for each 2 seconds of data sample.

Initially, measurements were made in the laboratory to test the code for column density retrieval with an infrared light source of 12 V powered glowbar. It was clear that in the field higher intensities of light shall be considered, however the light source provided enough light for the tests.

Glow bar was positioned 13.8 cm away from off-axis parabolic mirror. The mirror was colimating the beam in a perpendicular direction, directing it straight to the parabolic mirror of the instrument, whereas this mirror focused the beam to hit the sensor after transmission through the filter wheel.

Laboratory Measurements

In laboratory setup dark current was tested as a function of temperature. For lowering temperature a sack of ice water mixture was held in close proximity of the sensor heat sink. For highering temperature of the sensor a heat fan was used to blow warm air onto the heat sink of the seansor from a distance of approximately 50 cm. The following graph represents crystal clear correlation between the two physical properties of the sensor.

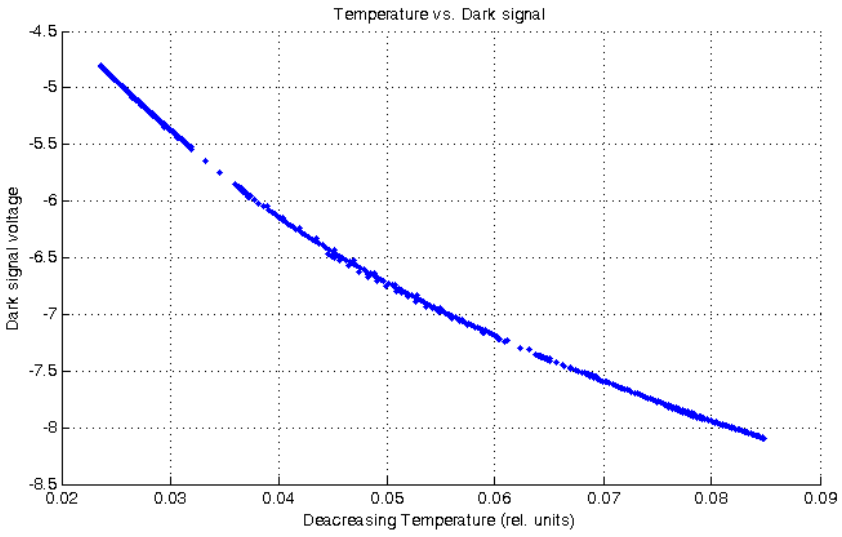

Figure 24 The dark signal dependance on temperature.

The test was run several times with varying voltages of amplifier power supply. By retrieving the correction from the inverse problem of the data, previously conducted experiemnt results were corrected, it yeald more than 10 times decrease in variability of dark current fluctuations, thus, finally justifying the hypothesis, that the variations in dark current channel over time of measurement is caused by large from variations in temperature of the sensor.

Solar Measurements

Measurements in Solar light were conducted on several days to test the long term stability of intestrument. Attention should be paid that long term stability of was interesting only for testing evaluation of solar zenith angle influence on column density calculations. Eventually the instruement should achieve stability of measurement within 15 minutes – maximum approximate plume traversing timespan.

The following case study was conducted around noon 12:40 to 13:57 on 3rd of June. The noon measurement is presented here as it has minimum influence from solar zenith angle change, thus rendering the measurement base line most stabile (figure 25).

Correction for the slope

The slope in measurements is expecteed mainly due to:

- Wavelength dependent sensor sensitivity,
- Scattering in the atmosphere (increasing with time in the afternoon).

The slope was corrected for implementing the reference filters by calculating the absorption in Reference 1 filter with respect to Reference 2 implementing the absorbance.m file, which contains algorythm:

A = -log10((((signal-dark)./(reference-dark))./ median((((signal(refrange)-dark(refrange))).(reference(refrange)-dark(refrange))))))

In identical manner the uncorrected Alkane 1 and Alkane 2 absorbances are calculated with respect to Reference 2 filter. Then, accounting for the distances in central wavelengths a linear exrapolation is done to determine the slope influence on both Alkane filters, and the slope influeced value is subtracted from measurement:

corr_AA2R2 = AA2R2 - R1toR2.*((306/99).^orderA2);

corr_AA1R2 = AA1R2 - R1toR2.*((204/99).^orderA1);

Thus, the above mentioned influences to the slope are minimized, however, there is obviously a component left uncompensated, this is due to non linearities in water absorption lines in the wavelength ranges of different filters.

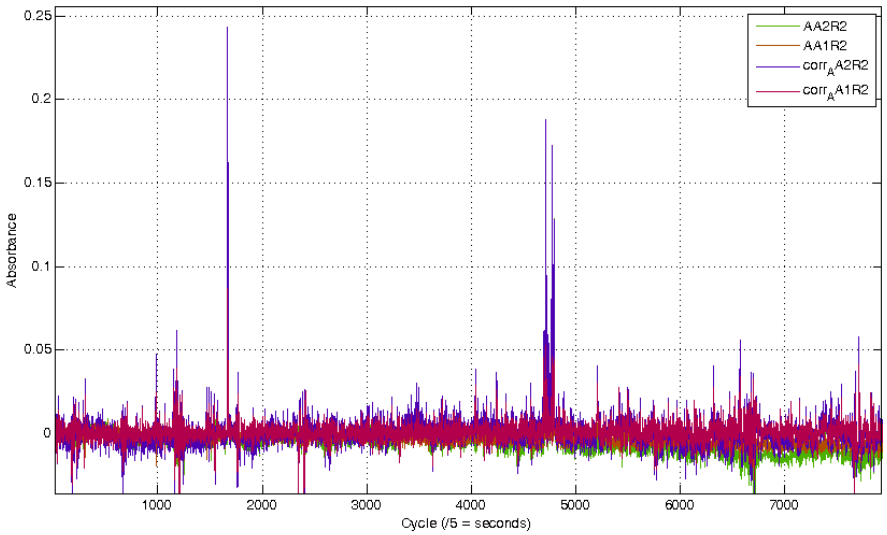

Figure 25 Alkane absorbance values for a stand still solar measurement with simulations of emission at 1700 and 4800 data points positions.

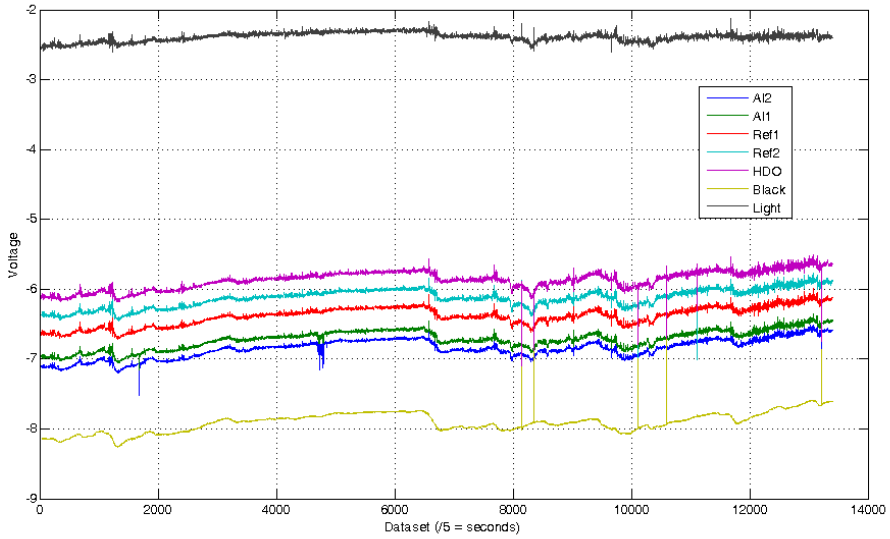

Figure 26 Example of voltage measurements over filter channels. Black is the dark, non-transparent filter signal. Light is the maximum voltage value within a cycle.

By observing the filter voltage levels simultaneously general stability of measurement series can be evaluated in the field. Thus, if sudden cahnges in filter signal levels or ratios is observed line should be able to relate this behaviour to external physical processes as wind speed increase (thus sudden temperature change) or absorbance pattern in alkane filters (plume presence), also maximum voltage change might signify of a cloud in the solar light path.

The peaks visible at about cycles 1700 and 4800 in the figure 25 are simulated emissions by using a propane/butane (70% / 30%) spray can.

In the figure 27 the simulated emission consists of many narrow peaks as for close

to the instrument plume simulation high column densities are observed, however, the gas is quickly carried away by local winds leaving basically no alkane concentration. For real emission plume measurements the lines are expected to be much wider or non existant.

For the emission simulation the cumulative absorbance graph was produced based on the slope corrected absorbance values.

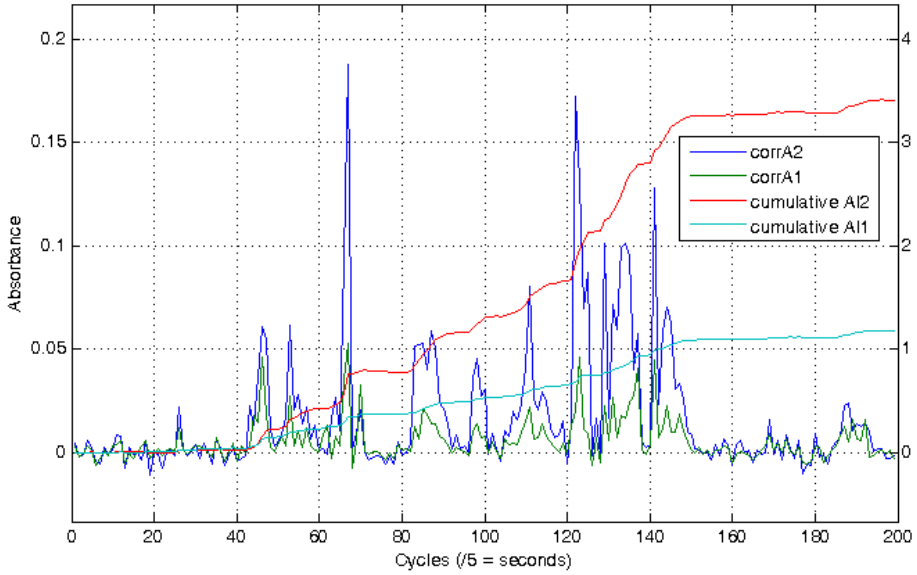

Figure 27 Emission simulation values corrected for the baseline slope and the corresponding cumulative absorbance graphs.

Knowing the cumulative values of absorbance the column densities further can be retrieved by dividing those by corresponding absorption cross sections for alkane filters.

The afternoon solar light measurements were significantly different from the noon measurement due to change in the solar zenith angle (SZA). As follows from Beer lambert law – the absorbance in a column is proportional to the pathlenght of light in the medium. As the Sun goes down the column increases and absorption of mainly water and methane is thereby increased. The following graph arose from measurements in the afternoon from 16:12 to 18:00.

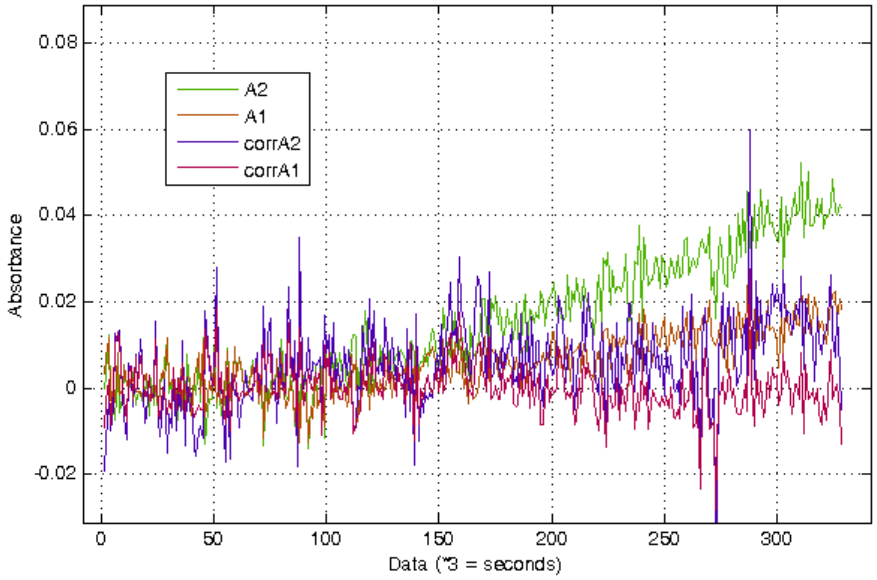

Figure 28 Illustration of afternoon drift in measurement baseline due to change in SZA for uncorrected and corrected measurements.

Field Measurement

The instrument was fixed on one plate with solar tracker and placed in an open trunk of a car. To secure stability solar tracker was strapped to the trunk. By driving as slowly as possible (approximately 10 km/h), measurements were condudted on one side of oil refinery. Real time graphical monitoring of results was organized also. Such valueas were monitored - channel voltage levels, calculated absorbances for Alkane 1 and Alkane 2 filters, current signal cycle graph, scatterplot between both alkane filter absorbance values, relative temperature and calculated carbon number. These graphs were satisfactory. GPS unit was launched parralel to measurements, recording time (synchronized with measurement time) and location of measurements.

Aspects differing from stand still conditions were - vibrations due to moving car and occasional shadow casting from light poles and cicyclisists passing by since measurement was done on the bicycle road.

Since only one field measurement campaign was organized, most of the time was spent avoiding troubles and readjusting instrument for precision operation. However, it was a success, since a plume was eventually captured. The following graph shows the plume alkane absorbances as calculated from both alkane filter measurements.

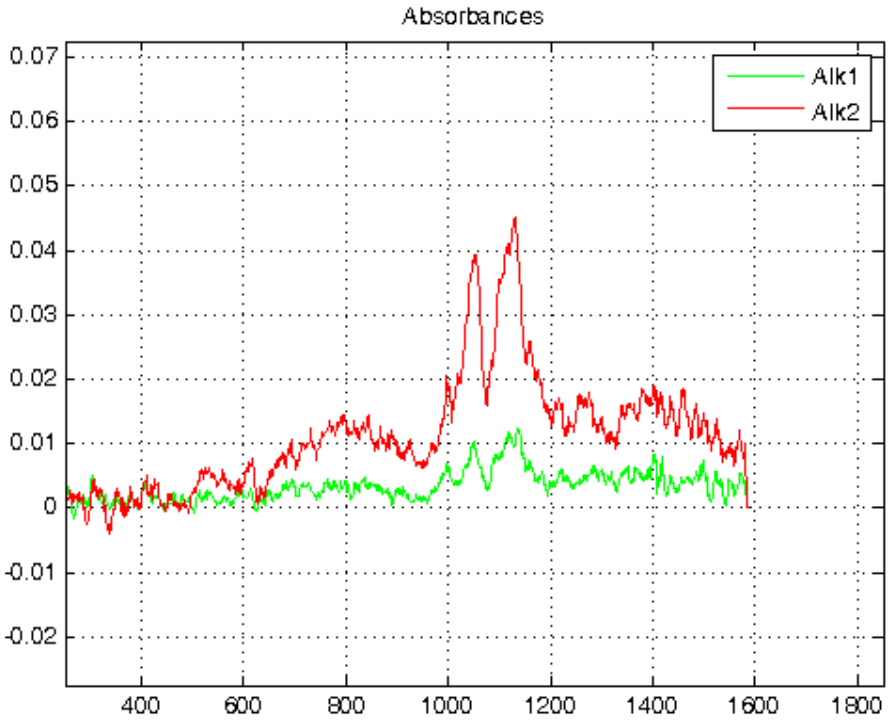

Figure 29 Plume alkane absorbance as measured in the field by two Alkane absorbance band filters.

Firstly, the carbon number is extracted from the absorbance measurements. As previously mentioned the linear correlation within bounds of 3 to 8 of carbon number versus (abosrption Alkane1) / (absorption Alkane2) were implemented. To add, the values, when absorption values, either Alkane1 or Alkane2, are less than 0.005 were removed from calculation matrices since at these conditions no carbon number estimation should be trustworthy as it disappears within measurement error or also could be that no significant column density of alkanes is present.

From in the field measurement the carbon number was estimated to be **4.6** which would signify of presence of heavier alkanes as pentane and/or hexane.

Emission rate estimation

When carbon number is known the values is rounded to a whole number and the corresponding cross section absorbances are assumed for the alkane mixture to evaluate the column densities and eventually flux. General expression of flux would be wind speed multiplication with cumulative column densities, in reality all values are varying with time – wind speed, speed of the car, columnd density, carbon ratio. However it is fair to assume values for the purpose of an estimate. Thus, my assumptions were:

Wind speed v – 4 m/s,

Car speed – 10 km/h,

Implementing the values in the following expression:

E1 = (36/10000)*sum(v.*ds.*A1)/(sigma_alk1);

Emissions was estimated to be 122 kg/h, where first brackets are unit conversion coefficient, sum brackets contain all time dependant wind speed *v*, increment of trajectory path *ds* for corresponding absorbance value measured *A1*, and *sigma* – absorption cross section retrieved through estimation of carbon number.

Simultaneously SOF measurements were conducted with a well established measurement technique. The results of the newly build instrument and high resolution spectrometer comply with each other.

8. DISCUSSION ON FURTHER DEVELOPMENT

The following aspects of the instrument are to be improved in the following work:

a. Sensor temperature stability and absolute temperature measurement,

b. Power supply converters to decrease variety of power sources,

c. Solar light incidence angle rectification,

d. Software improvements for robust performance,

Temperature stability has been monitored so far in relative units, and variability of temperature could be comparatively estimated between measurements by observing the error bar and its size relative to change of temperature median value. Absolute temperature monitoring would allow for more accurate tests for dependancies and eventual implementation of temperature corrections if necessary. Correcting itself might be unnecessary due to short measurement time intervals (15 minutes maximum).

Currently power supply is conducted by batteries for wheel rotation (1.5 V), bias voltage for sensor measurement (3 V), bias voltage for temperature measurement (9 V) and through a tripple power supply unit (~220 V) of symmetric +/- 12 V for signal amplifiers and 0.5 V for peltier element for thermoelectric sensor cooling. This speckled variety should be eventually reduced to single 12 V available from a car battery or a single 220 V chord. Though the power consumption from batteries is negligibe, the device should be running several months before exhausting battery power, once it will happen it might not be obvious in the measurement faults which one or several of batteries exactly have failed.

Solar light incidence angle onto the instrument is supposed to be strictly perpendicular, thus directing maximum amount of light onto the sensor. This is approximately this way right now, however, to yield maximum light efficiency some adjustments in instrument box position plane were necessary and performed. This

could be performed by achieving perfectly perpendicular incidence angle and then adjusting the parabolic mirror holder angle until the Sun spot picture on the filter wheel is perfectly circular.

Software performance should ultimately be improved by transforming the Matlab code into a fast performance and free language as C++. Since during taking measurements visual monitoring of the signal is highly necessary, the figure drawing can not be avoided for now. This slows down the code performance 2.5 times since figure drawing in Matlab is a memory consuming event.

Robustness of the code therefore must be improved in such aspect as possibility to run instrument even if there is not enough light (a thick cloud or a short term misoperation of Solar tracker).

REFERENCES

1. *Official Journal of the European Union, 30.04.2004, Directive 2004/42/CE of the EU and of the Council, p. 89.*
2. *Application of Solar FTIR spectroscopy for quantifying gas emissions, Manne Kihlman, 2005.*
3. *A non-dispersive instrument using the solar occultation flux method for gas emissions from volcanoes and industries, Beecken J., Borgentun C., 2007.*
4. *Wikipedia Benzene ring description, http://en.wikipedia.org/wiki/File:Benzene_Orbitals.svg, Novermber 2010.*
5. *CalSensors Inc. webpage, http://www.calsensors.com/*
6. *Hecht Opitcs, 2nd ed., Ch 9 Interference, p 333.*
7. *Mellqvist, J., et al., Measurements of industrial emissions of alkenes in Texas using the Solar Occultation Flux method, 2008JD011682, JGR, 2009.*
8. *Physical Principles of Remote Sensing, Gareth Rees, 2001, p 214.*
9. *VOC measurement workshop, Chalmers University of Technology, 2010-03-15.*
10. *Spring school on atmosphere-biosphere interaction with emphasis on eddy covariance, Kuopio University, Finland, 1st-5th March 2010.*
11. *Galle, B., J. Samuelsson, B.H. Svensson, and J. Börjesson. 2001. Measurements of methane emissions from landfills using a time correlation tracer method based on FTIR absorption spectroscopy. Environ. Sci. Technol. 35 (1): 21-25.*
12. *Open Path Fourier Spectrometry, Peter R. Griffiths, 2007, p 466.*
13. *Bo Galle, Development and Application of Methods based on DOAS and FTIR Absorption Spectroscopy for Atmospheric Research, Göteborg University, 1999.*

Appendix I

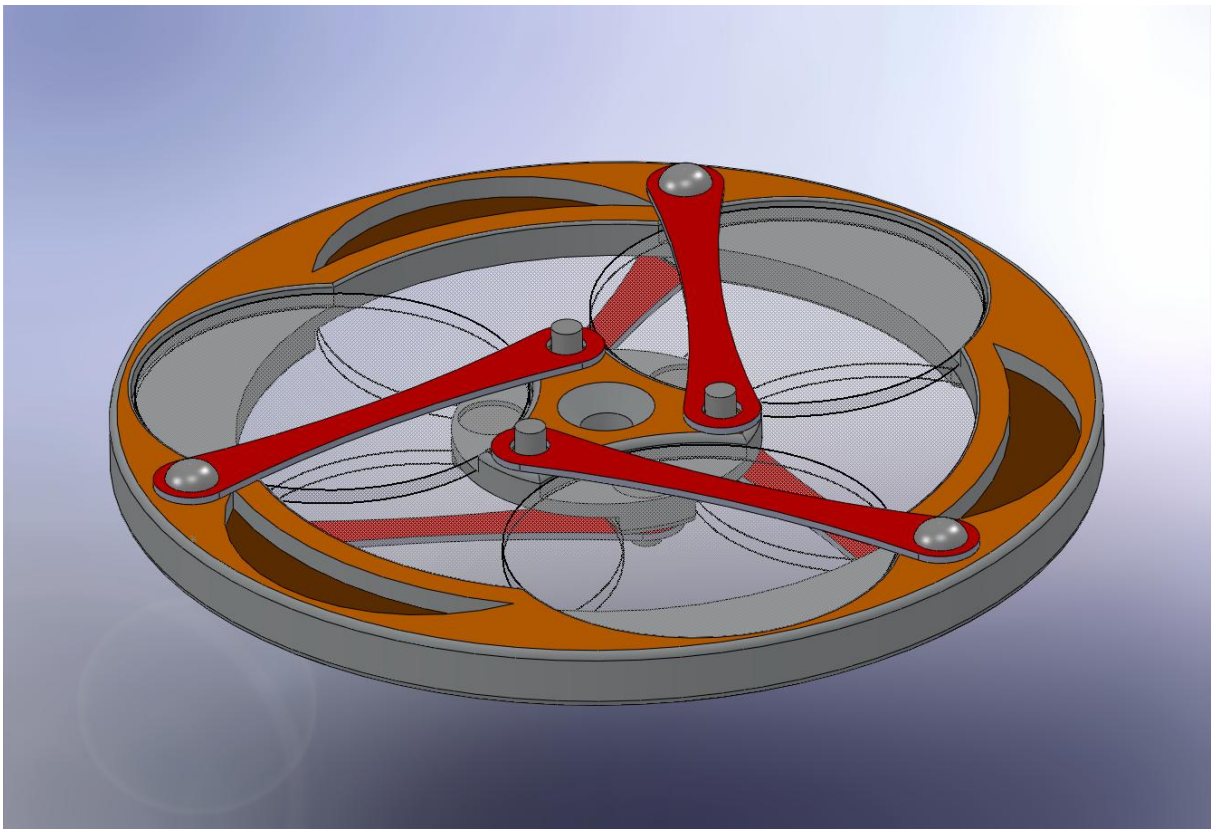

Figure 30 Discarded wheel design due to high complexity and high production costs.

Appendix II

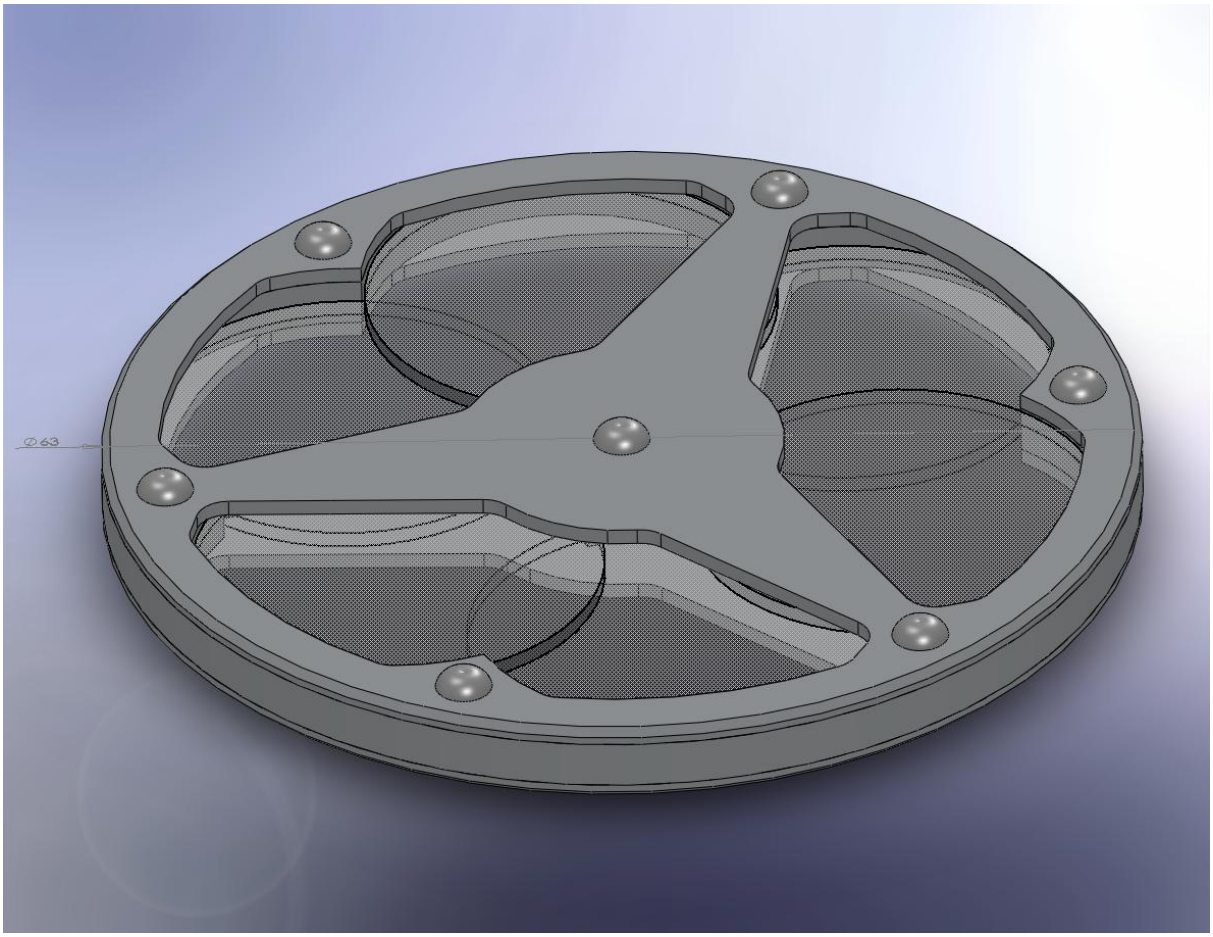

Figure 31 Final wheel design consisting of three different parts (without filters and screws).

Appendix III

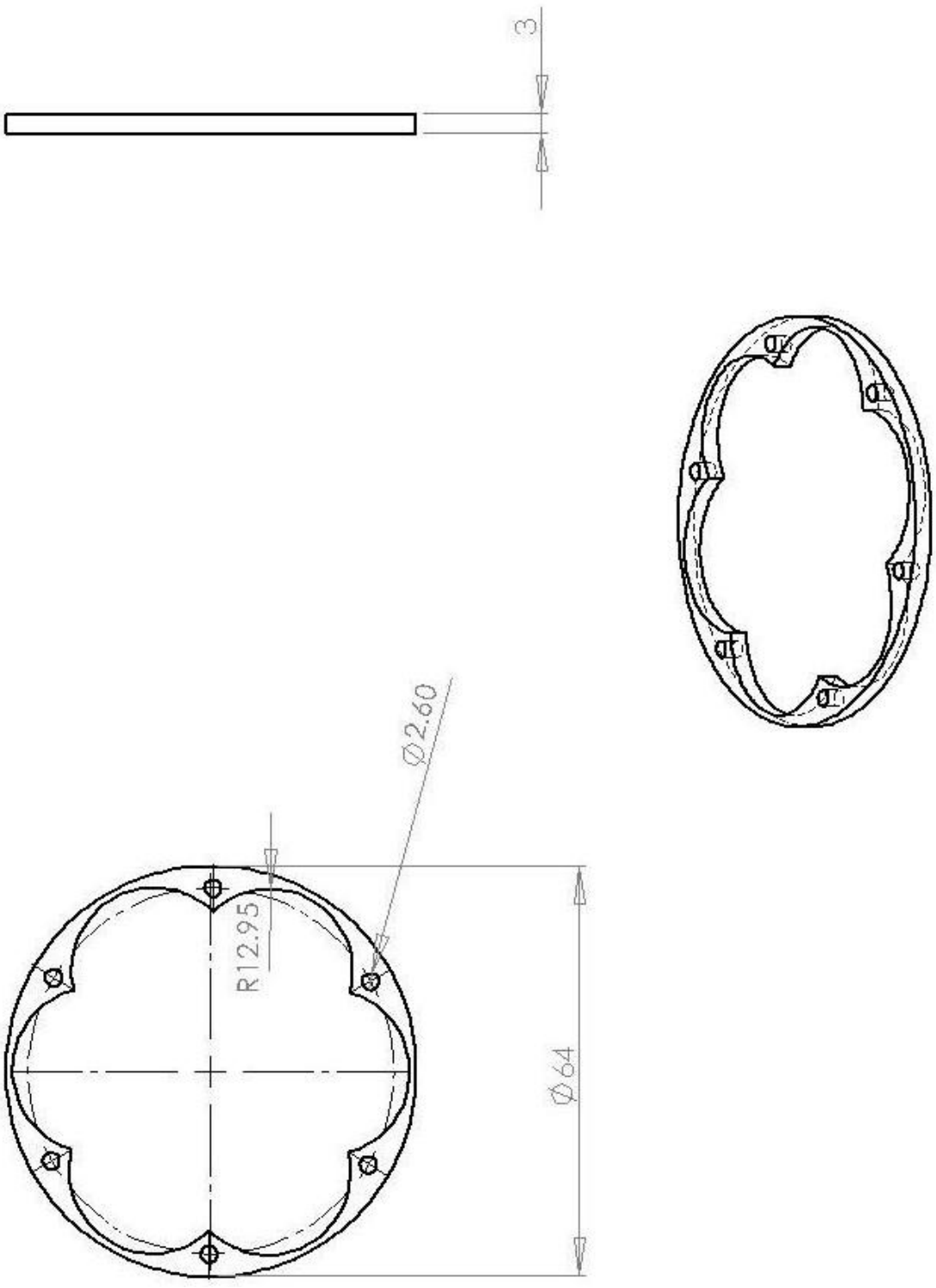

Figure 32 Outer wheel part.

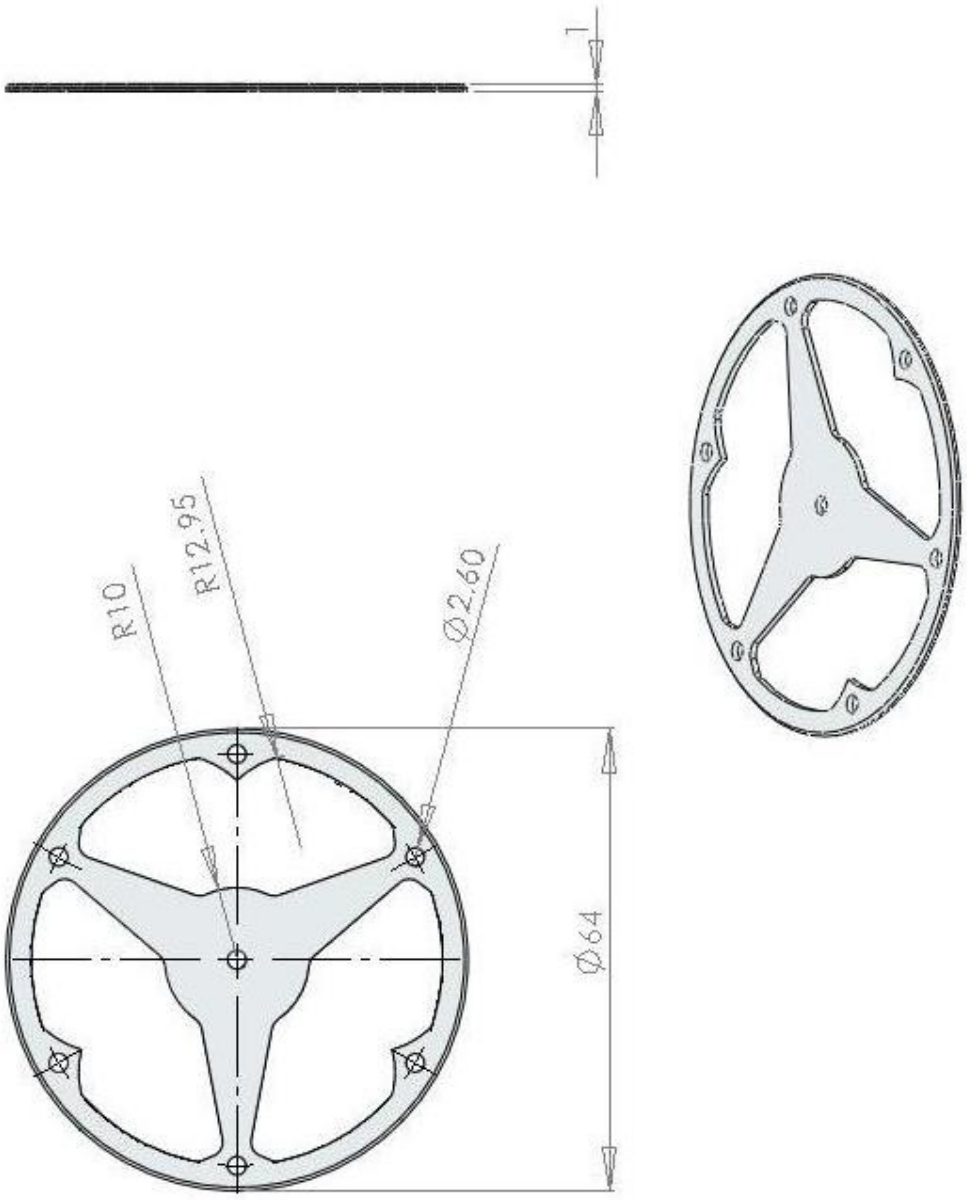

Figure 33 Top and Bottom wheel part. Two such parts are manufactured and placed on both sides of the Outer wheel part.

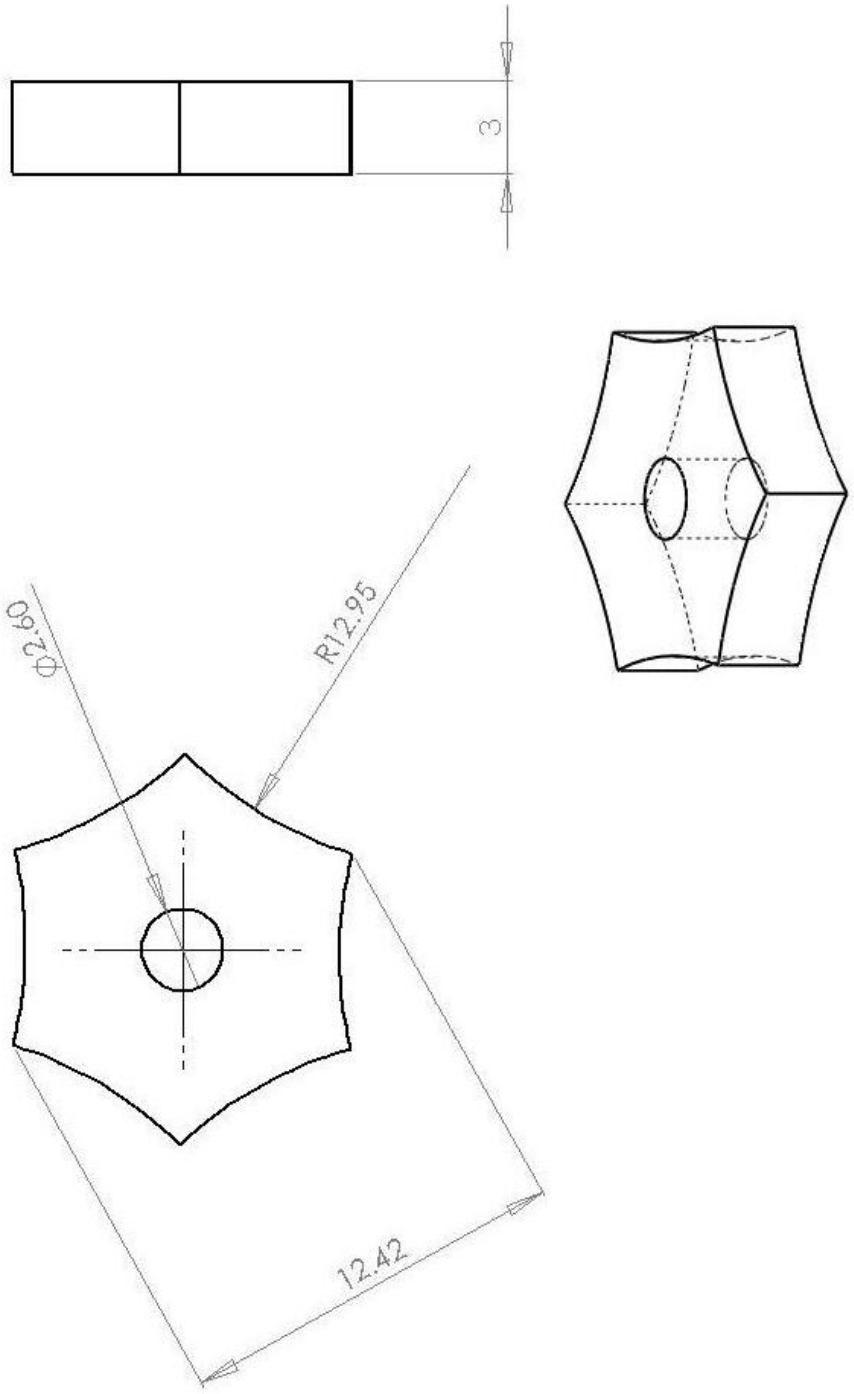

Figure 34 Center wheel part. Situated in the same plane as the Outer wheel part, placed in the center of the wheel, squeezed from both sides by Top and Bottom wheel parts.

Appendix IV

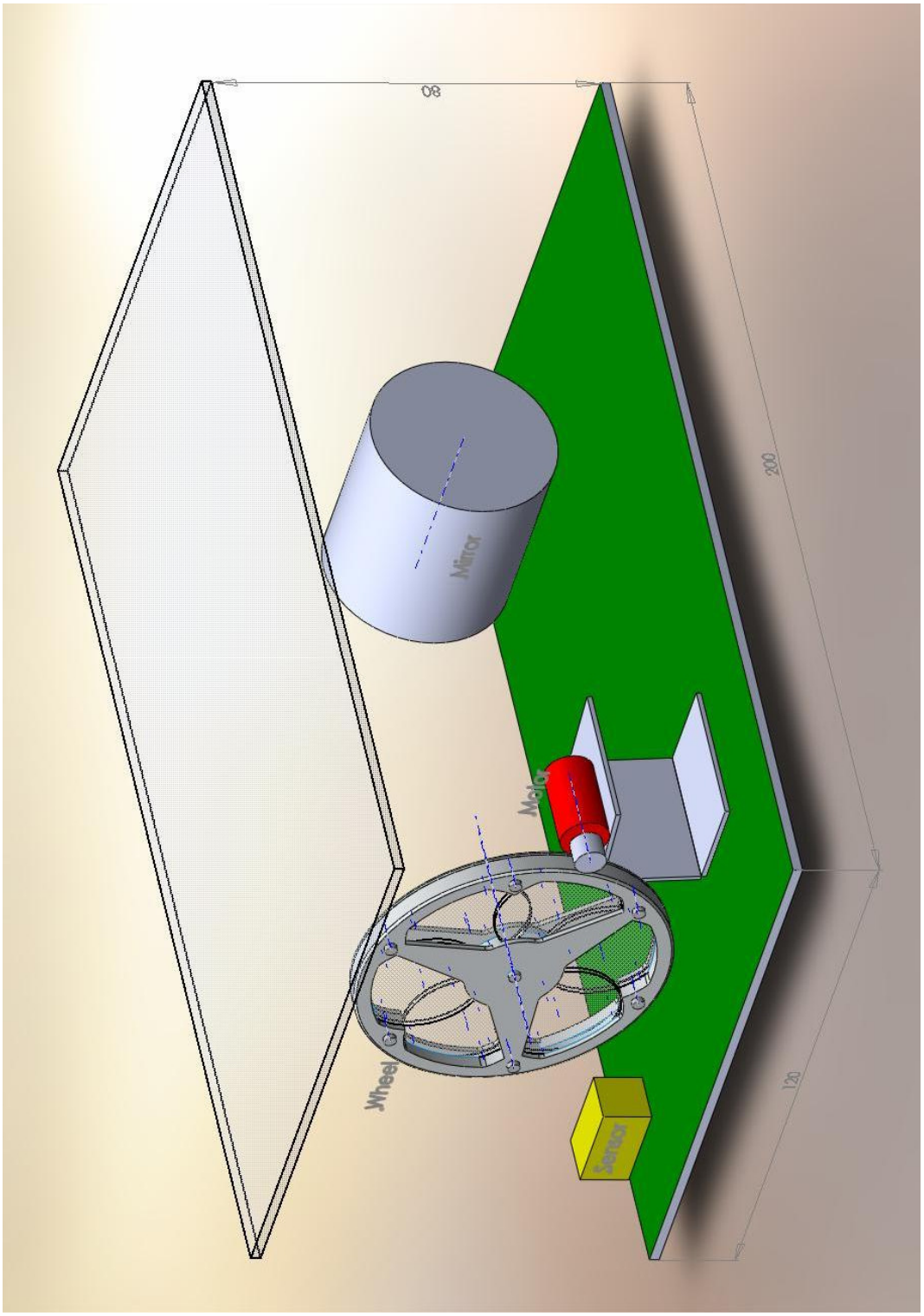

Figure 35 General design of device as modelled in Solid Works.

Appendix V

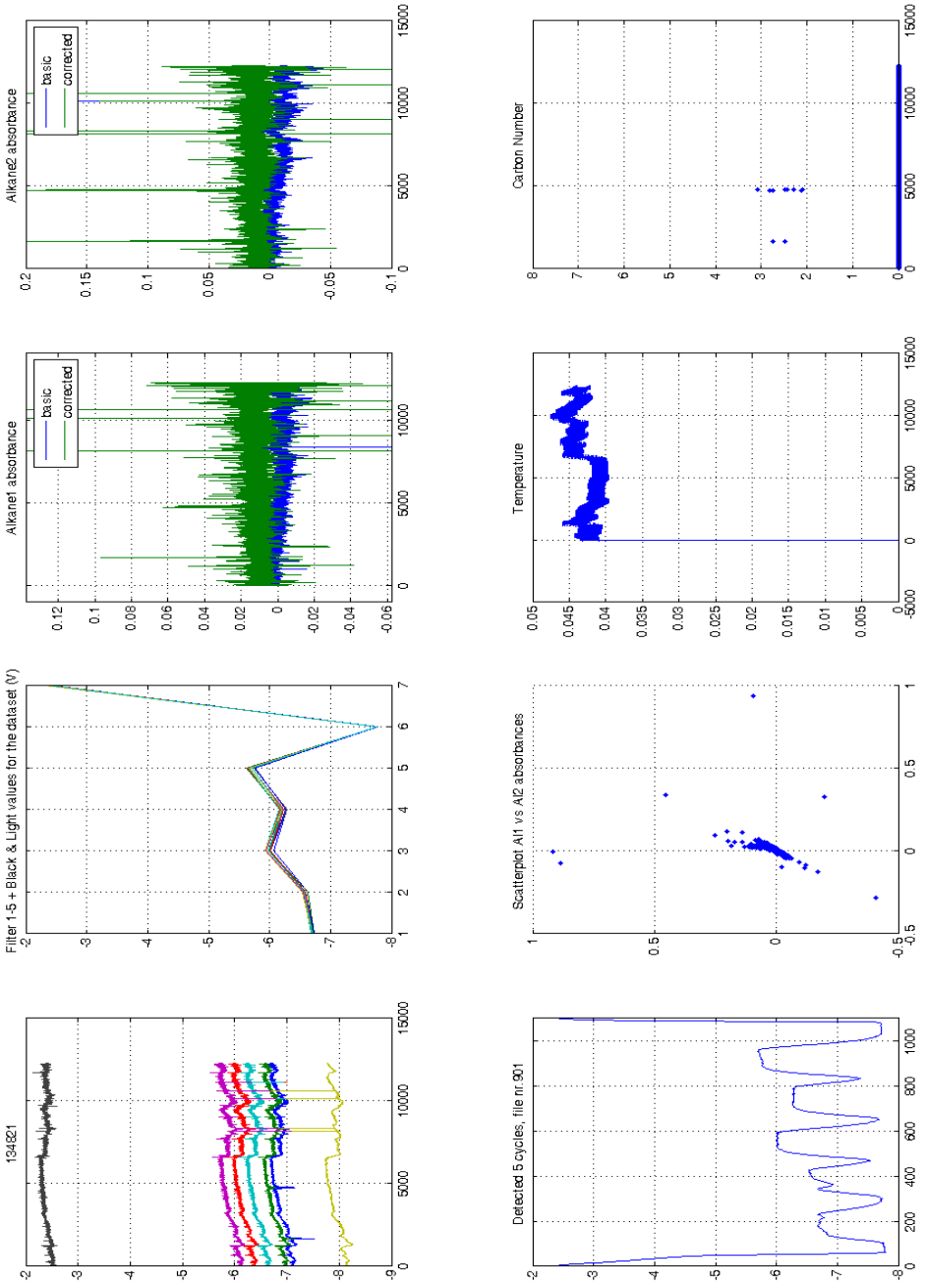

Figure 36 Measurement monitoring computer screen graph example.